CHAPTER IV
RESULTS

1. Preparation of compounds for biosynthetic studies

A. Chemical synthesis of [1-^{3}H]GGOH

[1-^{3}H]GGOH was synthesized from GGOH according to Section **2** of Materials and Methods. The diagram of [1-^{3}H]GGOH synthesis was shown in Fig. 19. The resulting [1-^{3}H]GGOH had its yield with the specific activity 0.028 Ci/mmol. The obtained label GGOH was identified by comparison its Rf value with the authentic GGOH. The synthesized [1-^{3}H]GGOH was used for synthesizing [1-^{3}H]GGMP and [1-^{3}H]GGDP by microsomal fractions of *Nicotiana tabacum* cell cultures.

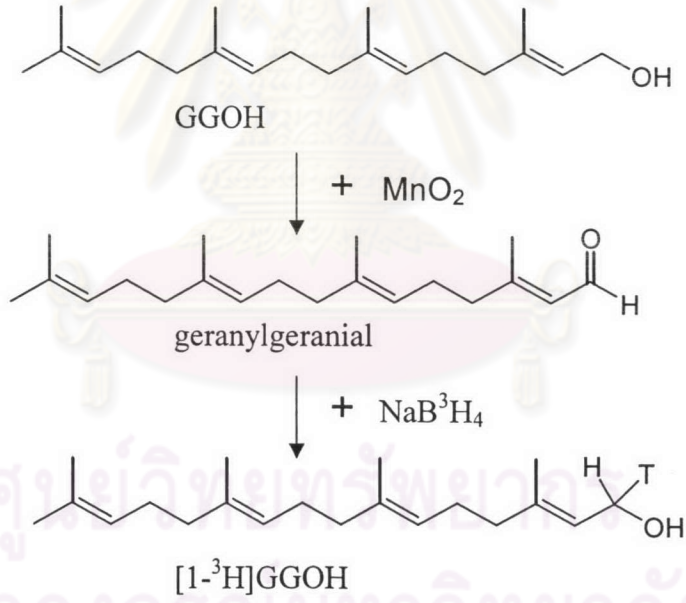

Figure 19 Diagram of chemical synthesis of [1-^{3}H]GGOH

B. Preparation of [1-^{3}H]GGMP and [1-^{3}H]GGDP by microsomal fractions

1. Detection of GGOH kinase activity

When [1-^{3}H]GGOH was used as the substrate and CTP was the phosphate group donor, kinase activities from microsomal fractions of both *Croton*

stellatopilosus cell suspension and *Nicotiana tabacum* cell suspension were detected and resulted to enzymatic products of [1-^{3}H]GGDP and [1-^{3}H]GGMP (Fig. 20). The enzymatic reaction steps were shown in Fig. 21.

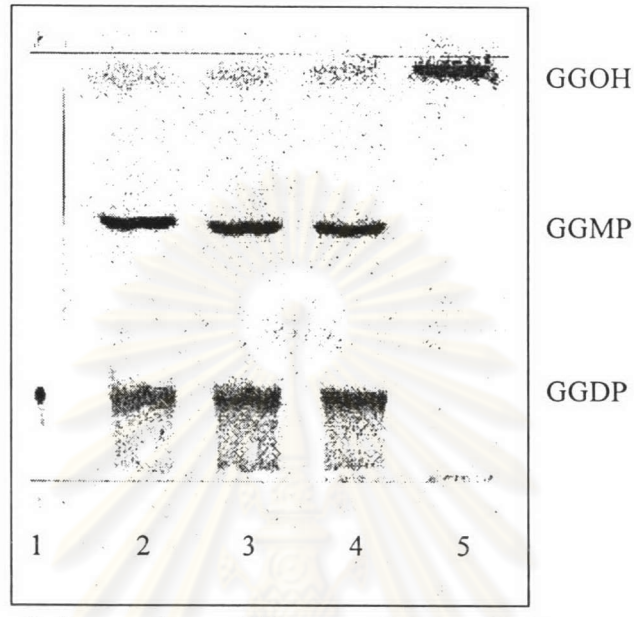

Figure 20 Phosphoimage showed kinase activities of microsome from *C. stellatopilosus*. :Lane1 standard GGDP (Iodine vapor), lane 2-4 reaction mixture, lane 5 control without CTP.

CTP appeared to be the phosphate group donor catalyzed by the microsomal kinase. No such kinase activity was detected with ATP, UTP, GTP, or ITP. It should be noted that the excess amount of microsomal protein could reduce GGDP formation. Overnight incubation of reaction mixture led to an appearance of various enzymatic products with significant loss of GGDP. The 100,000 x *g* supernatant of the same protein amount as microsomal protein showed no kinase activity. Also addition of more CTP, and enzyme after one-hour incubation did not give better yield of the labeled products.

2. Conditions for [1-^{3}H]GGMP and [1-^{3}H]GGDP formation

Attempts to increase the yield of [1-^{3}H]GGDP by the catalysis of microsomal kinases always resulted high formation of [1-^{3}H]GGMP as well. Since [1-^{3}H]GGMP is not commercial available and might also be an intermediate of dephosphorylation of GGDP to GGOH. We also aimed to obtain [1-^{3}H]GGMP for

this study. Based on the optimization, the highest yield of [1-^{3}H]GGMP appeared to be 95% from the reaction mixture containing 50 μg microsomal protein, 0.2 μCi [1-^{3}H]GGOH, 62.5 μM Tris/HCl pH 7.0, 6.25 mM CTP, 10 mM sodium orthovanadate, 5 mM $MgCl_2$ (Fig. 22A).

[1-^{3}H]GGDP was obtained with high yield under the same reaction mixture but using 62.5 μM MOPS pH 6.5 instead of 62.5 μM Tris/HCl pH 7.0. The yield of [1-^{3}H]GGDP was approximately 53-60% after one-hr of the incubation (Fig. 22B).

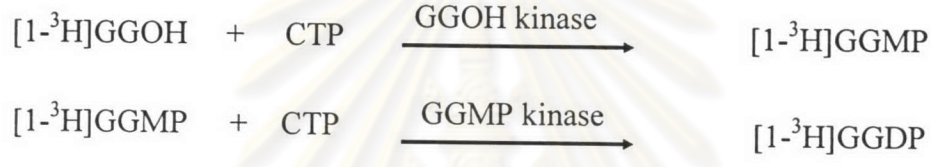

Figure 21 Diagram of enzymatic reaction of [1-^{3}H]GGMP and [1-^{3}H]GGDP formation from [1-^{3}H]GGOH.

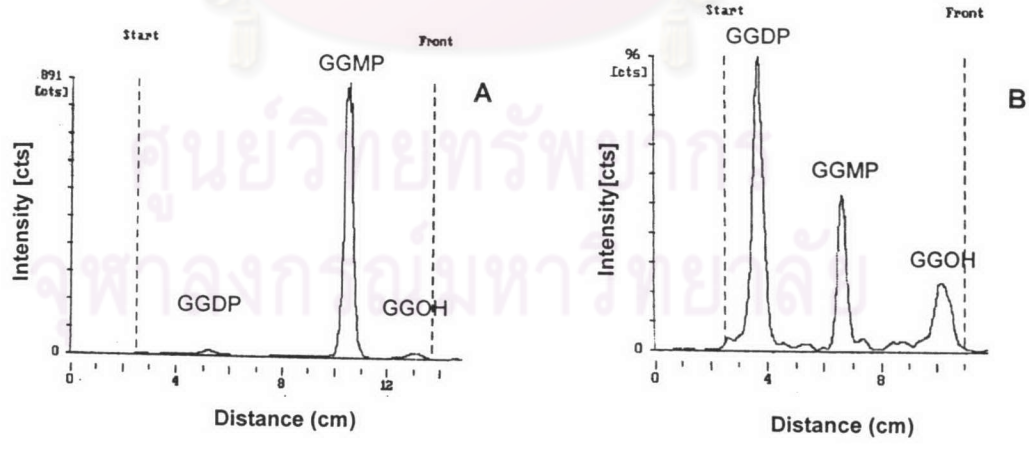

Figure 22 TLC radiochromatograms of enzymatic products from microsomal kinases. A) Enzymatic conversion of [1-^{3}H]GGOH to [1-^{3}H]GGMP with 95% yield under the condition of Tris/HCl buffer pH 7.0; B) conversion of [1-^{3}H]GGOH to [1-^{3}H]GGDP under the condition of MOPS buffer pH 6.5 with 53-60% yield.

3. Characterization and purification of [1-^{3}H]GGMP and [1-^{3}H]GGDP

The incubation of [1-^{3}H]GGMP (Fig. 23A), and [1-^{3}H]GGDP (Fig. 23B) with the alkaline phosphatase led to the formation of GGOH in both cases. No GGOH was detected in the control reaction mixtures without adding the alkaline phosphatase.

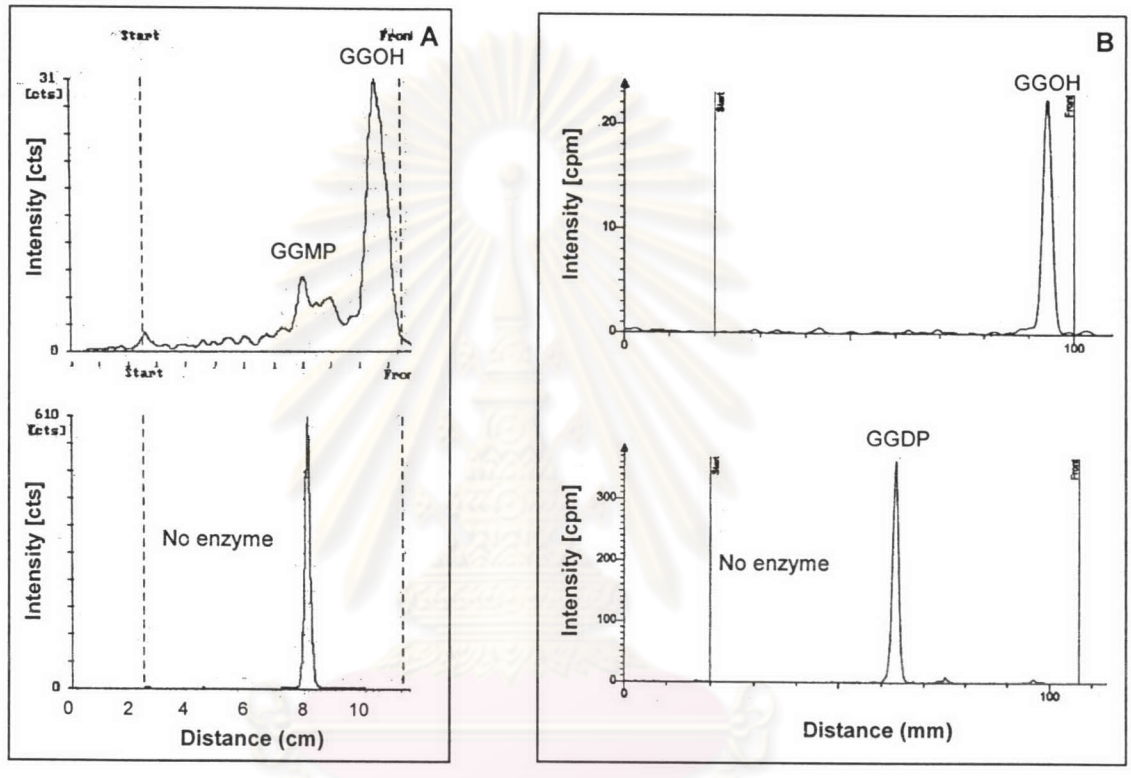

Figure 23 TLC radiochromatograms of dephosphorylation of [1-^{3}H]GGMP and [1-^{3}H]GGDP by alkaline phosphatase. A) Dephosphorylation of [1-^{3}H]GGMP to yield [1-^{3}H]GGOH as compared with no conversion in the absence of the enzyme. B) Dephosphorylation of [1-^{3}H]GGDP to yield [1-^{3}H]GGOH as compared with no conversion in the absence of the enzyme.

3. Purification of [1-^{3}H]GGMP and [1-^{3}H]GGDP

Higher scale of reaction mixture was performed to produce higher amount of GGDP. The 130-fold reaction contained 26 μCi of [1-^{3}H]GGOH. The extract after stopping reaction was concentrated and applied into MCI CHP20P column. The water-soluble substances of non-radioactive compounds were removed

by eluting column with 25 mM NH_4HCO_3. [1-^{3}H]GGMP, [1-^{3}H]GGDP, and [1-^{3}H]GGOH were eluted from the column at the concentration of 80%, 85-90%, and 100% MeOH in 25 mM NH_4HCO_3, respectively as shown in Fig. 24. [1-^{3}H]GGDP was obtained 2.27 μCi, or 8.7% from the starting amount of [1-^{3}H]GGOH.

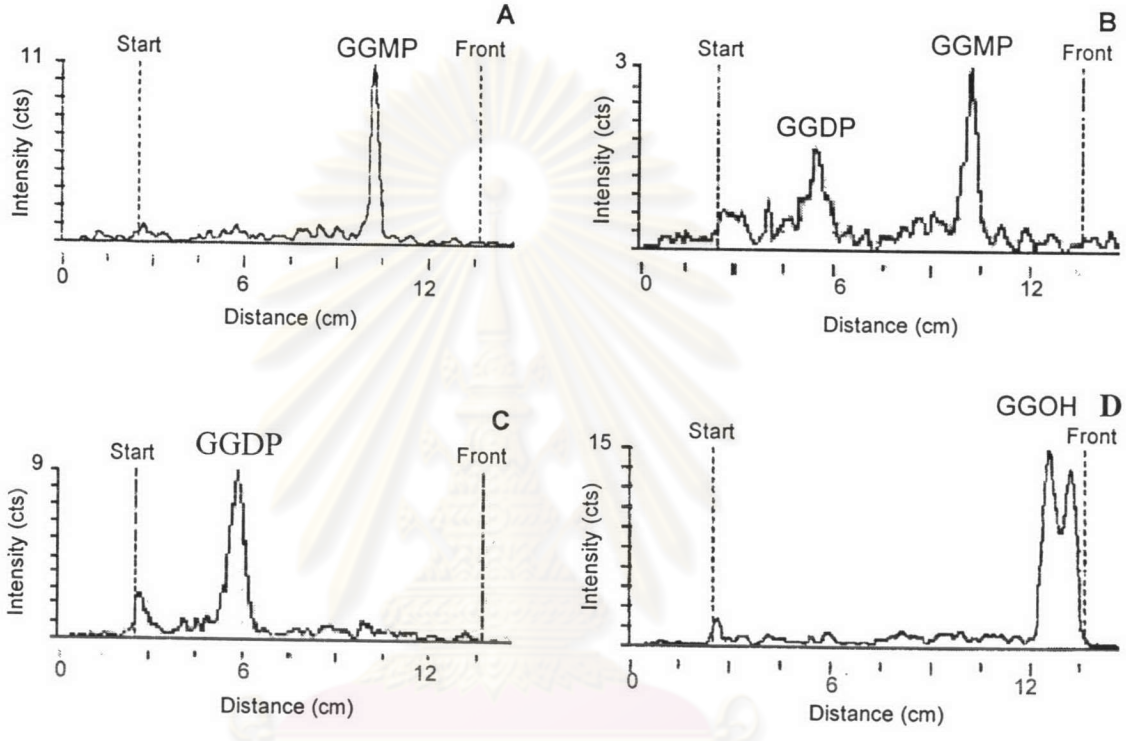

Figure 24 TLC radiochromatograms of the fractions from MCI gel CHP20P column, eluted with stepwise gradient of 25 mM NH_4HCO_3 and MeOH. A) GGMP fraction from 80% MeOH, B) mixture of GGMP and GGDP from 80% MeOH, C) GGDP fraction from 85-90% MeOH, D) GGOH fraction from 100% MeOH.

3. Chemical synthesis of dibenzoyl plaunotol

The reaction of dibenzoyl plaunotol synthesis was shown as follows (Fig. 25):

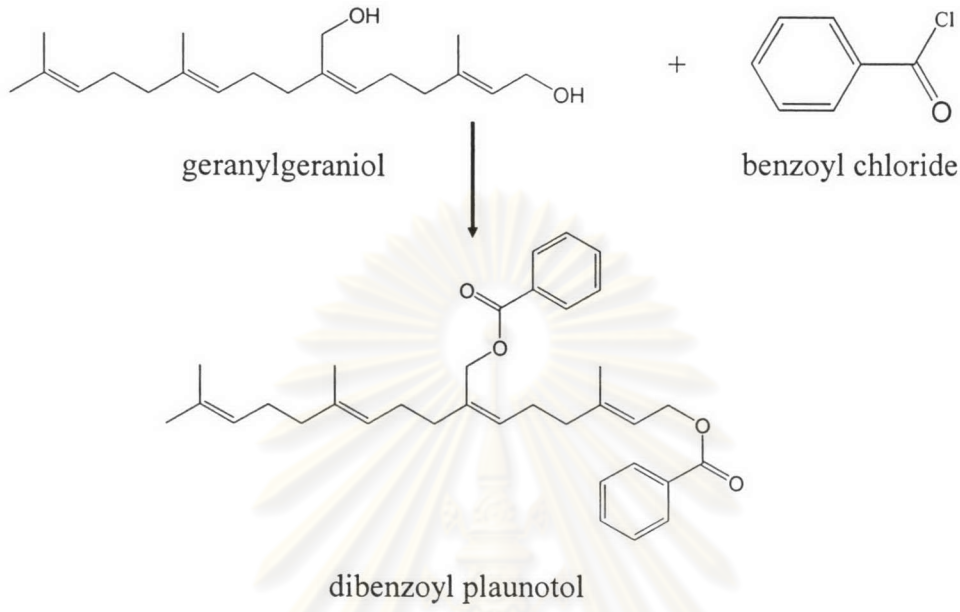

Figure 25 Diagram of chemical synthesis of dibenzoyl plaunotol

The structure of dibenzoyl plaunotol was confirmed by FTICR (Fig. 26). MW of plaunotol is 306, therefore the MW of 537 indicated two groups of benzoyl available in the structure.

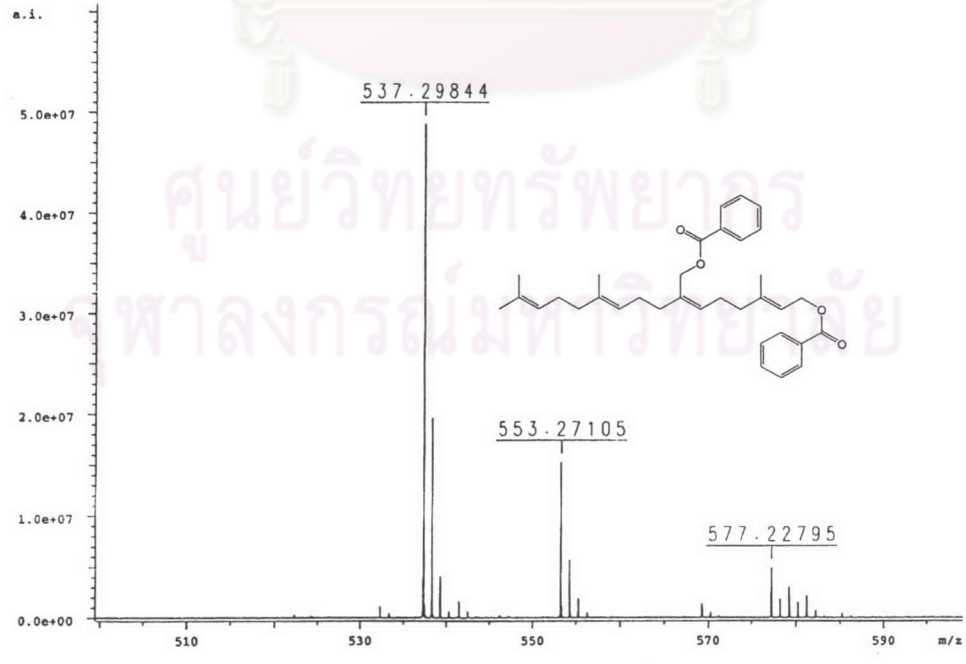

Figure 26 FTICR of dibenzoyl plaunotol ($C_{34}H_{42}O_4$) MW 514 + Na 23 = 537

2. Biosynthetic study of *C. stellatopilosus*

A. Feeding leaves of *C. stellatopilosus* with [1-^{3}H]GGOH

The healthy leaves were fed with 10 μCi [1-^{3}H]GGOH for 92 hours. Then they were extracted with 80% ethanol, and acid-base partitioned with $CHCl_3$ as mentioned in the method. The TLC radiochromatogram of $CHCl_3$ extract is shown in Fig. 27.

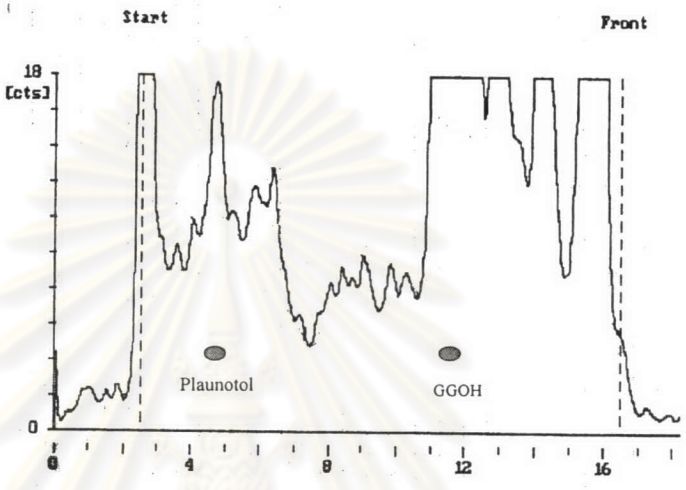

Figure 27 TLC radiochromatogram of $CHCl_3$ extract from leaf feeding with 10 μCi [1-^{3}H]GGOH compared with authentic samples which were detected by I_2 vapor (black spots)

The small amount of plaunotol was obtained from the feeding leaves. The plaunotol area were cut from a silica TLC plate, and eluted with EtOAc. The EtOAc extract of 4,690 cpm was mixed with plaunotol 500 μg (1.63 μmol) to synthesize a derivative with benzoyl chloride. The result is shown in Fig. 28. The chromatogram of the reaction mixture showed a few amount of dibenzoyl plaunotol.

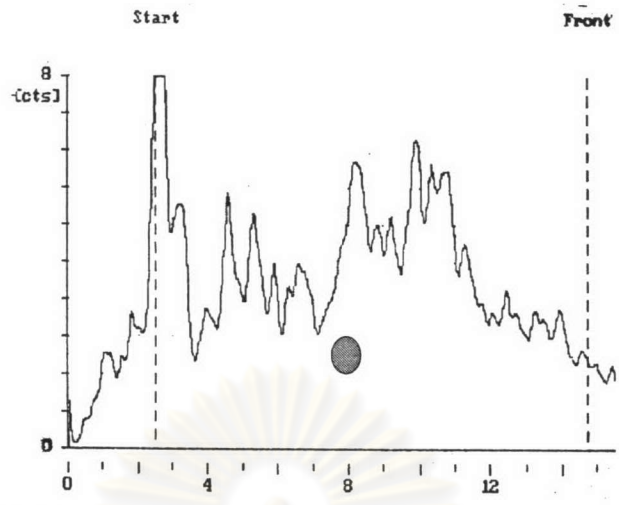

Figure 28 TLC radiochromatogram showed trace amount of a compound at the same Rf as the dibenzoyl plaunotol (spot). Standard of dibenzoyl plaunotol was detected under UV_{254} nm.

B. Feeding callus and cell suspension cultures of *C. stellatopilosus* with [1-^{3}H]GGOH

Cell callus and cell suspension cultures of *C. stellatopilosus* were fed with 10 μCi of [1-^{3}H]GGOH. After a suitable time, they were extracted with 80% EtOH, and were partitioned with chloroform as decribed in Method. The chloroform extract was applied to a silica gel TLC plate, solvent system of benzene-MeOH (9:1). The phosphoimage of TLC is shown in Fig. 29.

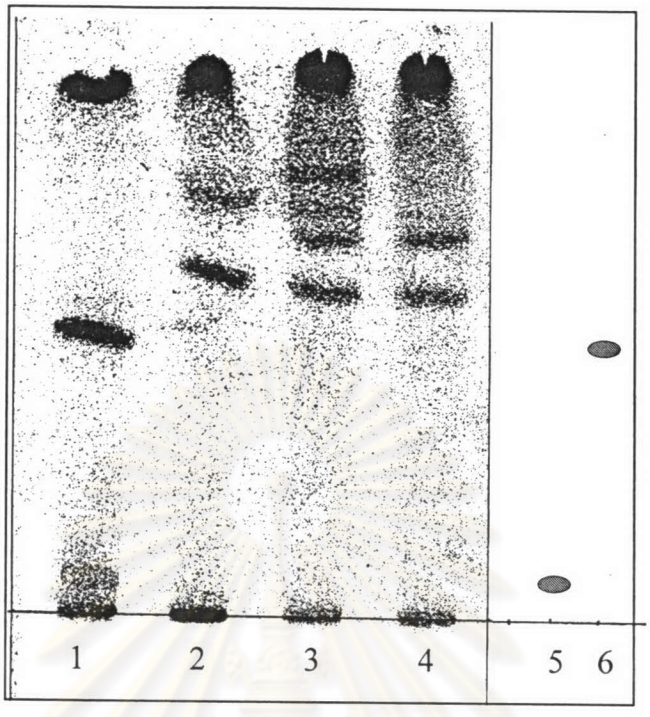

Figure 29 TLC phosphoimage of callus and cell suspension of *C. stellatopilosus* fed with [1-^{3}H]GGOH. Lane 1: callus; lanes 2-4; cell suspension; lane 5; plaunotol; lane 6: geranylgeraniol. (lane 5 and 6 were detected with iodine vapor.)

The TLC chromatogram of callus and cell suspension fed with [1-^{3}H]GGOH showed the major product at the front of TLC. This substance was not further identified. The callus feeding show one band at the same Rf value of plaunotol, but its amount was too small to be detected by derivatization. The result showed clearly that feeding of cell suspension did not produce plaunotol.

C. Detection of GGDP phosphatase activity in cell-free extract

1. Detection of GGDP phosphatase activity in chloroplast of *C. stellatopilosus* leaves

Chloroplast was extracted from fresh leaves of *C. stellatopilosus* by sucrose gradient (Fig. 30). The layer between 30% - 40% sucrose was used for GGDP phosphatase assay. The results were shown in Fig.31 and Fig. 32 that GGDP and GGMP were dephosphorylated into GGOH. GGMP was detected as intermediate of dephosphorylation from GGDP into GGOH.

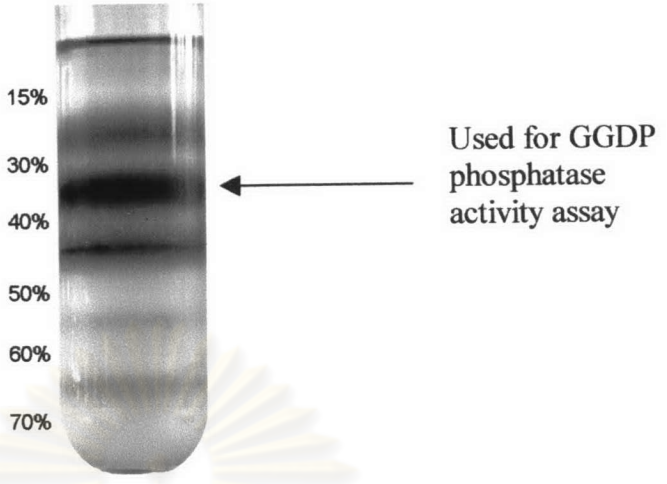

Figure 30 Sucrose gradient for chloroplast separation from *C. stellatopilosus* leaves

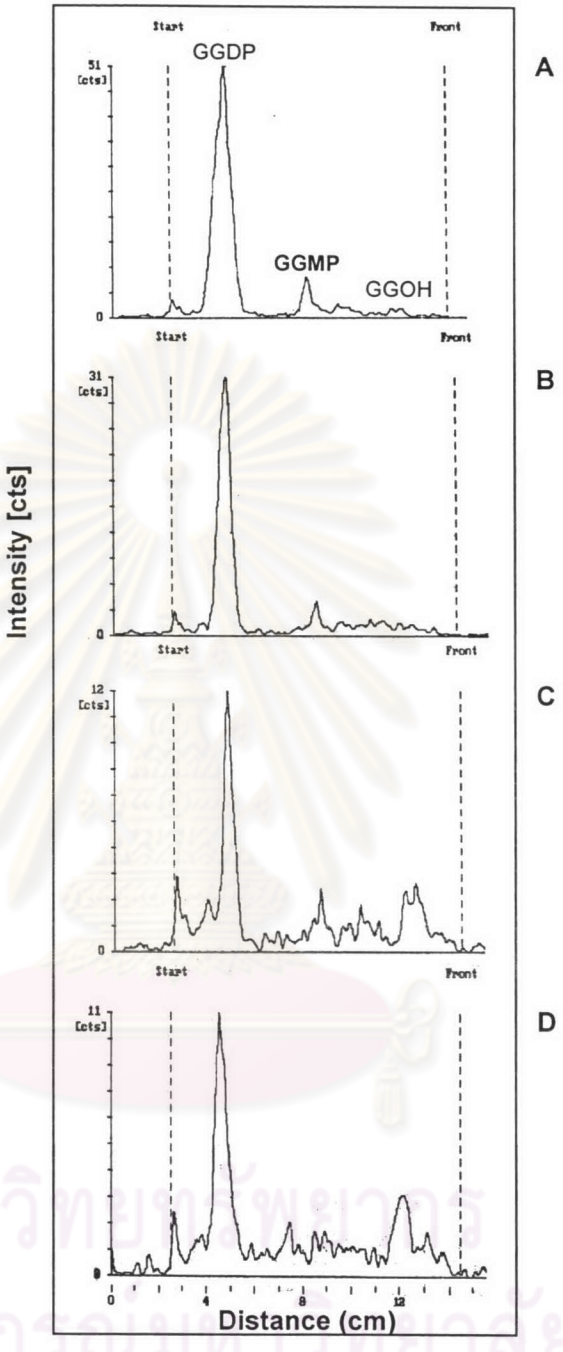

Figure 31 TLC radiochromatograms of GGDP phosphatase activity of chloroplast extract of *C. stellatopilosus*. A) assayed with chloroplast in chlorophyll concentration of 30 μg/μl; B) assayed with chloroplast in chlorophyll concentration of 50 μg/μl; C) assayed with chloroplast in chlorophyll concentration of 100 μg/μl; D) assayed with chloroplast in chlorophyll concentration of 150 μg/μl.

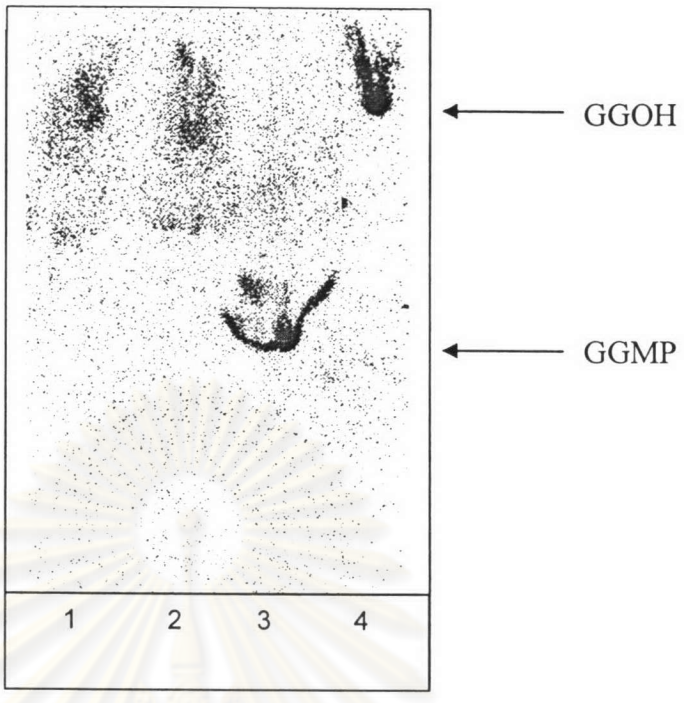

Figure 32 Phosphoimage of GGMP phosphatase activity in the chloroplast preparation of *C. stellatopilosus.* Lane 1-2: assay with [1-^{3}H]GGMP as substrate; lane 3: boiled control; lane 4: [1-^{3}H]GGOH.

D. Detection of GGDP phosphatase activity in 20,000 x *g* fraction of *C. stellatopilosus* cell-free extract

The pellet fraction obtained from 20,000 x *g* and its supernatant were detected for GGDP phosphatase activity compared with the boiled control and the reactions without GGDP. All reactions were incubated for 30 min at 30 ^{O}C using Tricine buffer pH 7.8. The resulting TLC detected by Iodine vapor (Fig. 33) showed the presence of GGOH peak in both the pellet and the supernatant fractions. No such a peak in the presence and the reaction mixture without substrate. The typical TLC densitochromatogram at 210 nm of the 20,000 x *g* pellet fraction is shown in Fig. 34.

These results were consistent to the previous report (Tansakul and De-Eknamkul ,1998) showed the presence of both the GGDP phosphatase and GGOH 18-hydroxylase in 20,000 x g pellet. Therefore, the pellet fraction was chosen for further investigation.

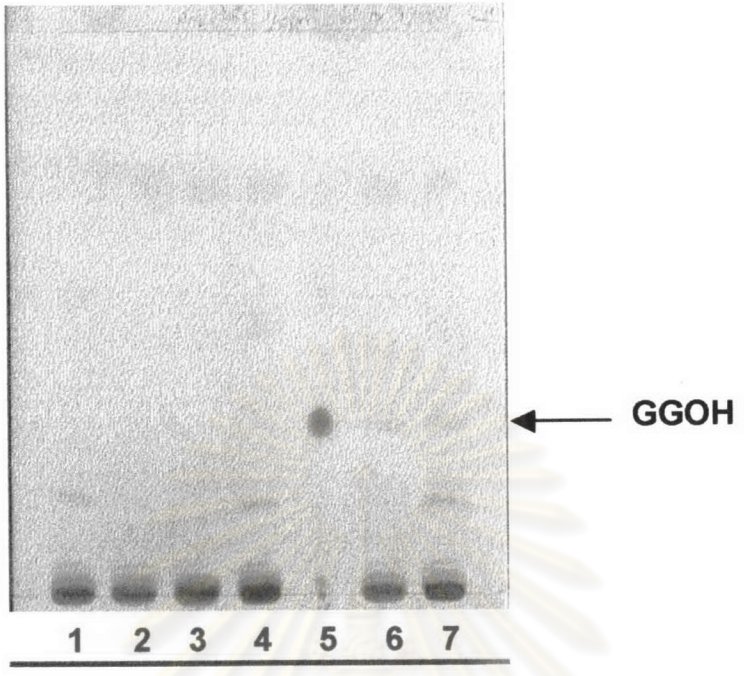

Figure 33 TLC patterns of products obtained from GGDP phosphatase activity in 20,000 x *g* fraction of *Croton stellatopilosus* leaves. The reaction mixture contained 67 μM GGDP, 100 mM Tricine buffer pH 7.8, and 100 μl desalted enzyme preparation. Lane 1: pellet without GGDP; lane 2 supernatant without GGDP; lane 3: supernatant boiled controlled; lane 4: pellet boiled controlled; lane 5 GGOH (Sigma); lane 6: supernatant with GGDP; lane 7: pellet with GGDP.

E. The effect of triton X-100 solubilization on the membrane-bound GGDP phosphatase.

The green crude GGDP phosphatase obtained from solubilized 20,000 x g pellet with 0.1% Triton X-100 followed with 100,000 x g centrifugation for 60 min, its supernatant was the crude GGDP phosphatase. As shown in Fig. 35, the crude GGDP phosphatase desalted by PD-10 column exhibited the activity as same as the 20,000 x *g* pellet, that meaned Triton X-100 can solubilyzed all of membrane-bound GGDP phosphatase. The precipitate from 100,000 x *g* centrifugation showed trace of GGDP phosphatase activity due to some supernatant contamination to the pellet. The result from Fig. 35 clearly indicated that GGDP phosphatase is a membrane-bound enzyme.

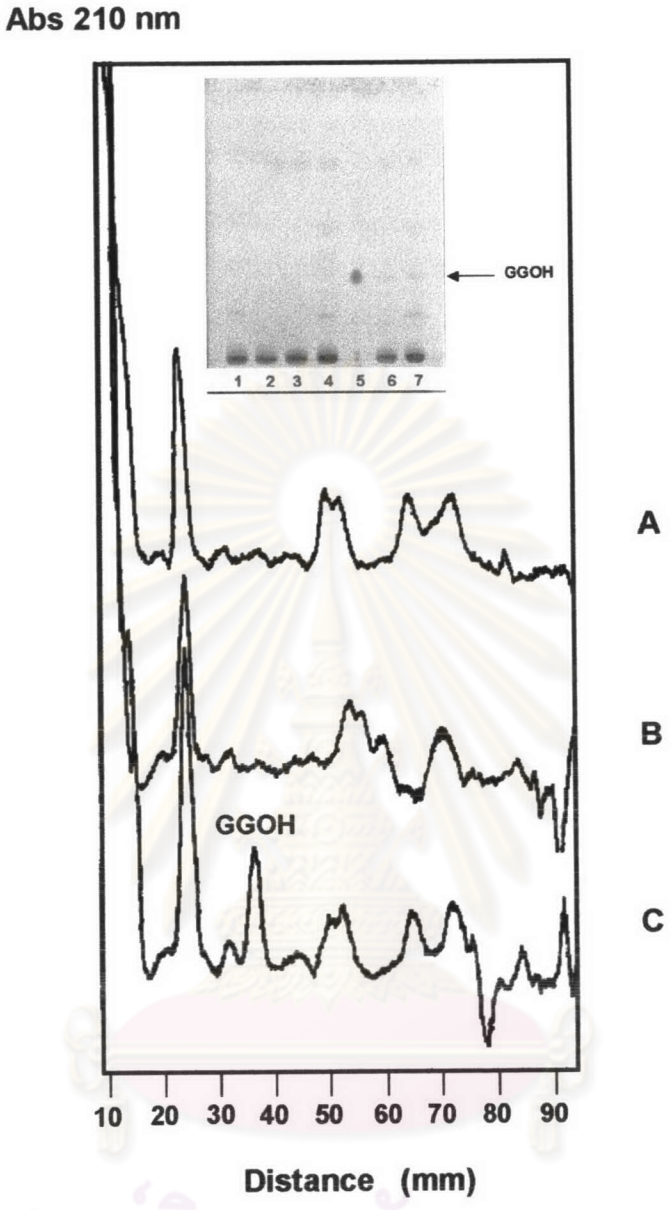

Figure 34 A typical TLC-densitochromatogram of the reaction mixture (λ_{210} nm) detected from the TLC plate as shown in Fig. 33 (insert).
A) Boiled control (lane 4); B) 20,000 x g pellet without substrate (lane 1);
C) 20,000 x *g* with GGDP (lane 7).

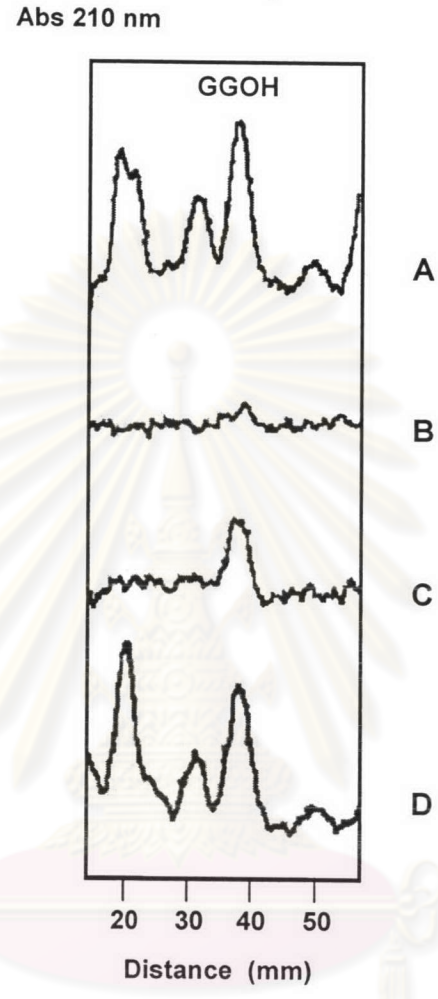

Figure 35 TLC-densitochromatogram showing the activity of GGDP phosphatase before and after membrane solubilization. A) Non-solubilized pellet 100,000 x *g*; B) supernatant 100,000 x *g* without detergent; C) Solubilized-pellet 100,000 x *g*; D) supernatant 100,000 x *g* after solubilized.

3. Purification and characterization of GGDP phosphatase from *C. stellatopilosus*

1. Optimization of GGDP phosphatase assay

Preliminary studies on the properties of the solubilized crude GGDP phosphatase was carried out in order to design the optimum condition for enzyme activity assay and for the planning of enzyme purification steps. The desalted crude GGDP phosphatase was determined for its optimum pH and buffers. The results showed that the best buffer for the enzyme assay was Tris/HCl pH 7.0.

Under this condition, the reaction mixture containing 67 μM GGDP, 0.5 M Tris/HCl pH 7.0 at 30 ^{O}C showed GGOH formation in the linear relationship with time for up to 60 min. The optimum temperature of incubation was performed in various temperatures from room temperature to 100 ^{O}C. The result as shown in Fig. 36 indicated that the GGDP phosphatase activity was observed at 50 ^{O}C.

For enzyme stability study, the enzyme preparation was kept at 4 ^{O}C and –20 ^{O}C for up to 45 days and was determined periodically for its activity. As shown in Fig. 36 the enzyme activity at 4 ^{O}C storage appeared to be decreased until lost all activity within 10 days, whereas at –20 ^{O}C storage, the enzyme activity still remained with no significant loss. We, therefore design the purification step in refrigerator within one day, after that we can store the enzyme preparation in –20 ^{O}C for a long time throughout the experiment.

From this preliminary study, the standard conditions for enzyme assay was optimized as follows: 150 μl reaction mixture containing 67 μM GGDP, 0.5 M Tris/HCl pH 7.0, 60 min incubation time at 30 ^{O}C. The enzyme was stored at –20 ^{O}C and could be freezed and thawed for several times.

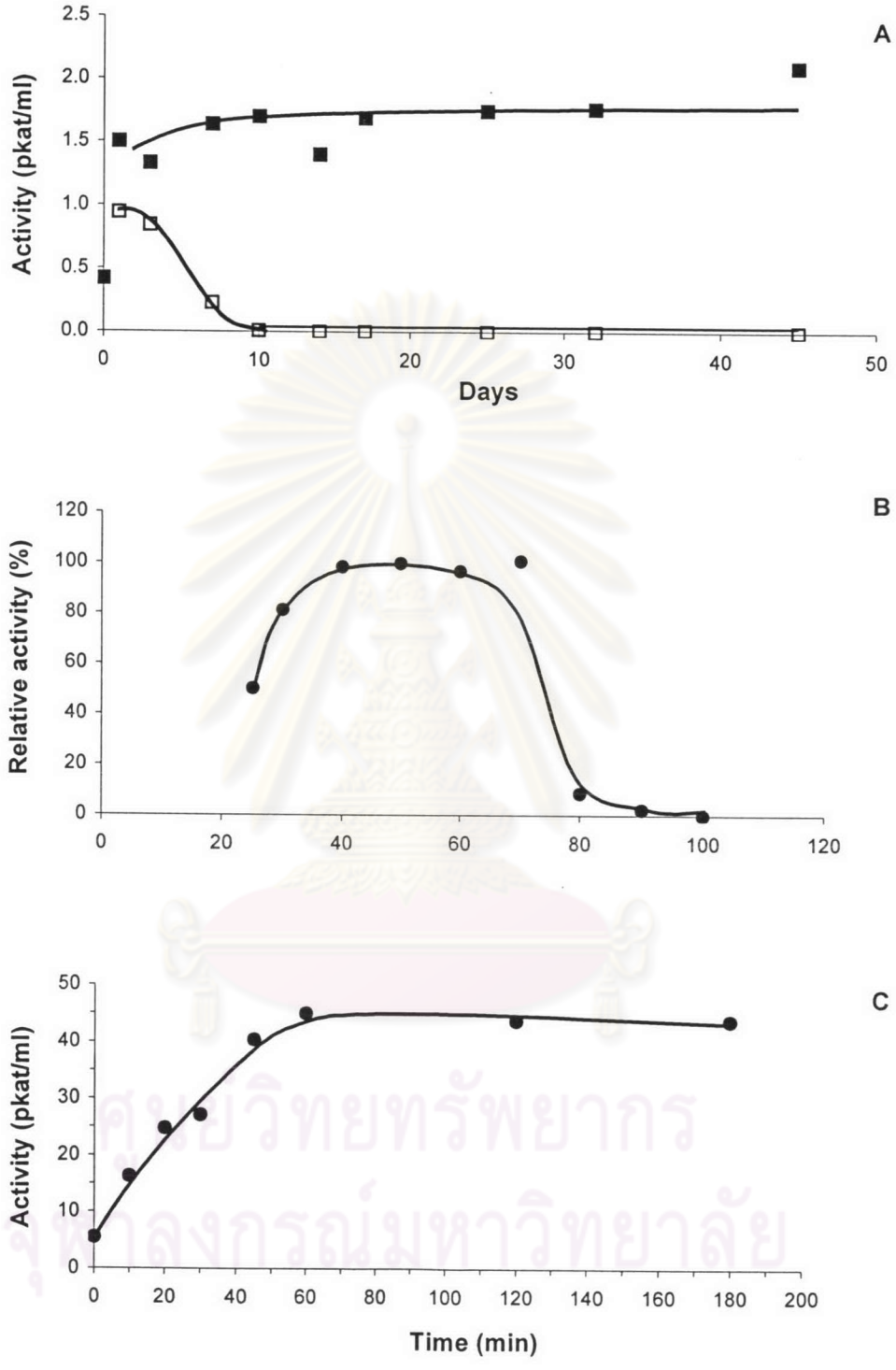

Figure 36 Optimization of GGDP phosphatase assay. A) Stability of the crude GGDP phosphatase storage in –20 ^{O}C (■); and 4 ^{O}C (□); B) optimum temperature of the crude GGDP phosphatase activity; C) time-course of the crude GGDP phosphatase activity.

2. Purification of the solubilized GGDP phosphatase

Fresh leaves which were not too young and not too old were collected. The crude GGDP phosphatase extract was obtained as described in Section **3** of Materials and Methods. The crude enzyme extract concentrated and desalted by using Centriprep-30 (Amicon) was firstly pass through a gel filtration column of BioGelA. The chromatogram of the BioGelA column was shown in Fig. 37.

PI and PII were concentrated separately by lyophillization into a small volume. Each of them was loaded on to a Sepharose 6 gel filtration column. The protein pattern from this column was cleaner and showed one major band on SDS-PAGE gel. The major peak of PI from the Superose 6 column with GGDP phosphatase activity (Fig. 38) was used to determine for native molecular weight. The active PII fraction from the BioGelA column was also lyophyllized and applied on the same Superose 6 column (Fig. 39). The major peak with GGDP phosphatase activity was determined for native molecular weight using this calibrated column. The active peak fraction of PII from the Superose 6 column was lyophilized to reduce its volume. It was then applied to the UNO Q anion exchange column (Bio-Rad) (Fig. 40). The column was eluted with 20 mM Tris/HCl and NaCl gradient from 0-1 M. The active fractions were pooled and were dialyzed against the resuspension buffer. It was again concentrated by lyophillization and checked for purity by SDS-PAGE with silver staining, but the protein from the UNO Q column could not be detected due to trace amount of the obtained protein. The SDS-PAGE of the enzyme preparations from various steps of purification was shown in Fig. 41. The summary of GGDP phosphatase purification was shown in Table 7. The purification of P I was 3.1 fold from Superose 6 column, whereas the purification of PII was 157 fold from Superose 6 column and 274 fold by UNO Q column.

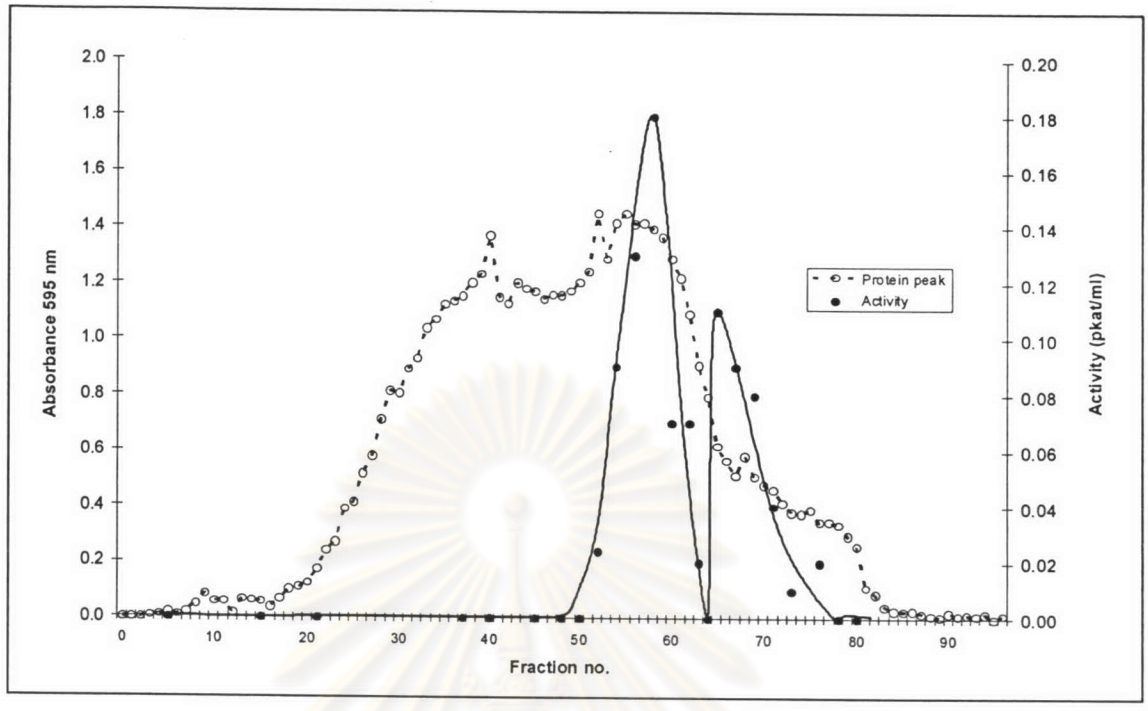

Figure 37 Chromatogram obtained from BioGel A column chromatography of crude enzyme extract. ● GGDP phosphatase activity, ○ protein

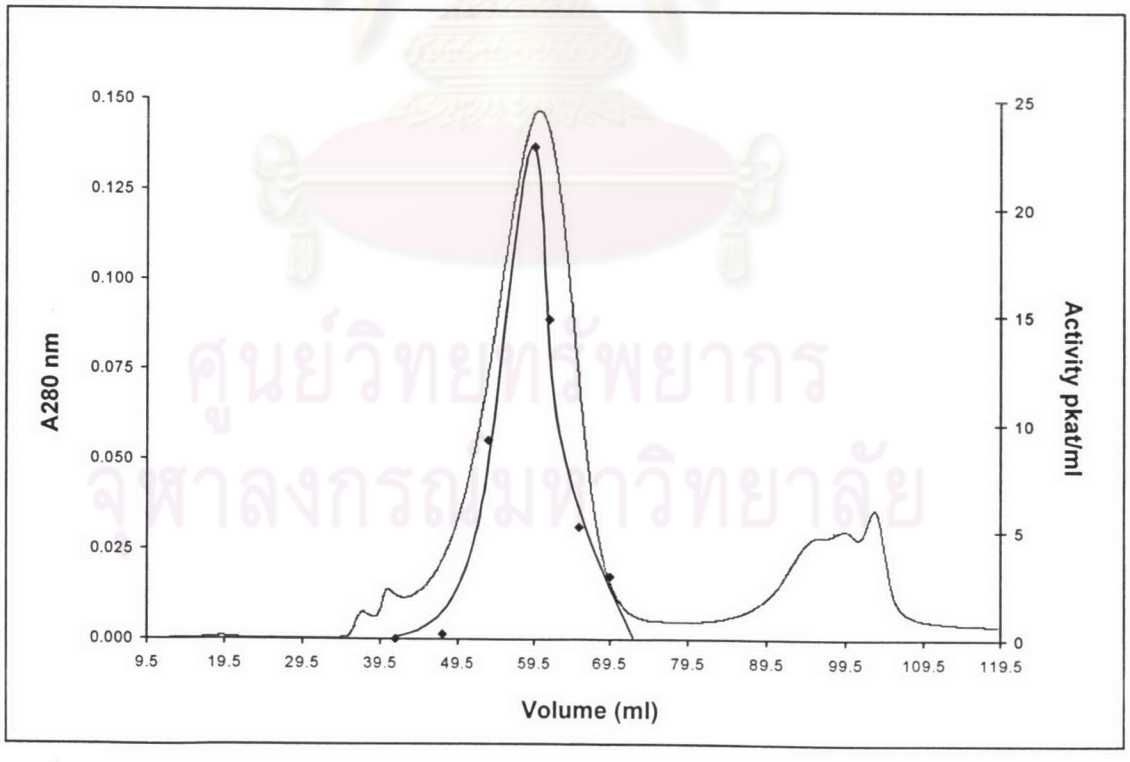

Figure 38 Chromatogram of PI separation by Superose 6 column.

(—— : protein absorbance at 280 nm; ♦: GGDP phosphatase activity)

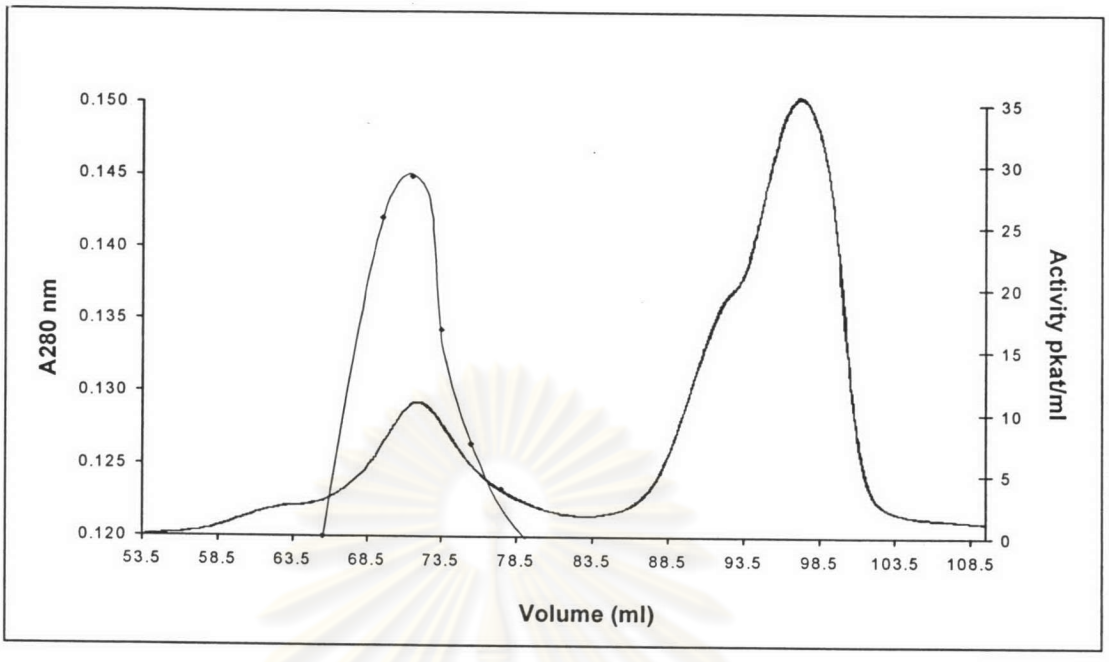

Figure 39 Chromatogram of PII separation by Superose gel column

(—— : protein absorbance at 280 nm; ♦: GGDP phosphatase activity)

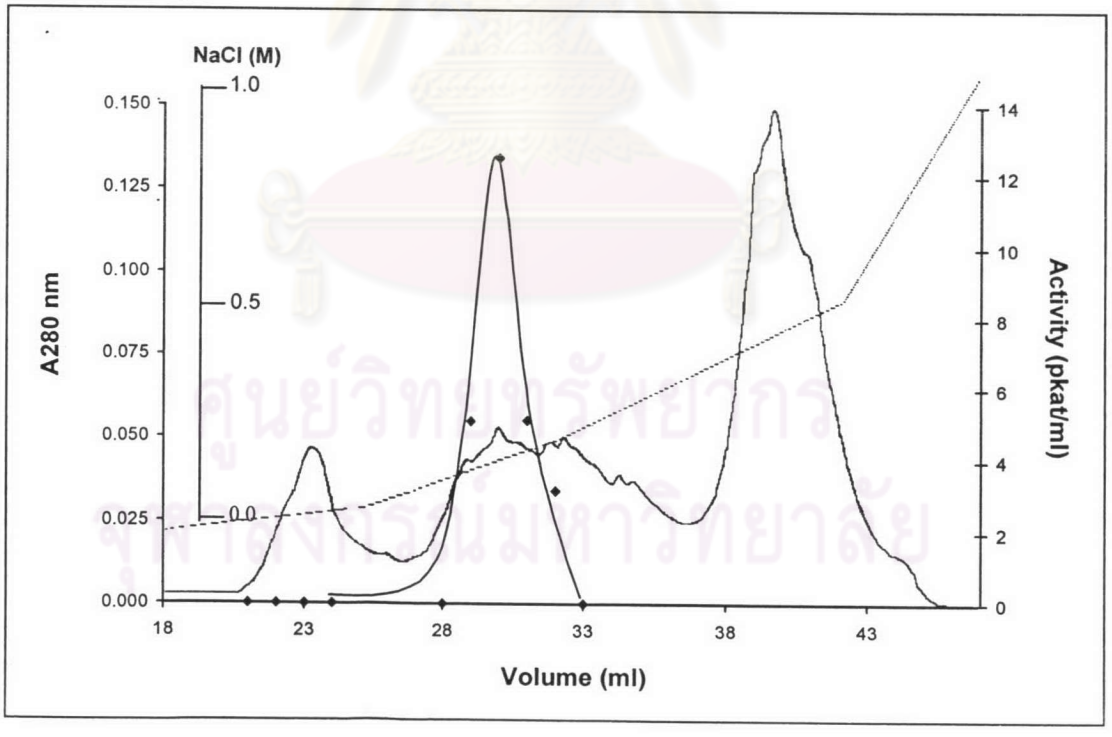

Figure 40 Chromatogram of PII separation by UNO Q column

(—— : protein absorbance at 280 nm; ♦: GGDP phosphatase activity;

-·-·- : NaCl concentration(M))

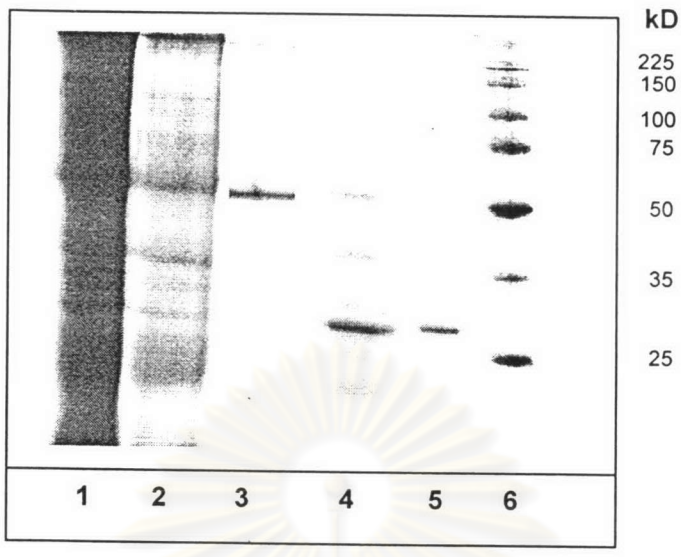

Figure 41 SDS-PAGE of various enzyme preparation obtained during enzyme purification of PI and PII from *Croton stellatopilosus*. (Lane 1: crude GGDP phosphatase; lane 2: PI fraction from the BioGel A column; lane 3: PI fraction from the Superose 6 column; lane 4: PII fraction from the BioGel A column; lane 5: PII fraction from the Superose 6 column; lane 6: molecular weight maker.

Table 7 Summary of GGDP phosphatase purification from *C. stellatopilosus* leaves

Purification step	Volume (ml)	Total protein (μg)	Total activity (pkat)	Specific activity (pkat/mg)	Yield (%)	Purification Factor (-fold)
Crude extract	114	59875	1263.8	21.1	100.0	1.0
BioGel A						
PI	25	13535	401.8	29.7	31.8	1.4
PII	20	1161	563.8	486.0	44.6	23.0
Superose 6						
PI	50	3940	261.5	66.4	20.7	3.1
PII	12	86	285.7	3322.0	22.6	157.4
UNO Q						
PII	6	8	45.5	5786.8	3.6	274.2

3. Molecular weight determination

3.1 Determination by SDS-PAGE

The enzyme preparations of PI and PII were subjected to SDS-polyacrylamine gel electrophoresis. After running, the gel was developed with coomasie blue. The molecular weights of PI and PII were estimated with comparison their relative mobilities (Rf) to those of known molecular weights of the broad range protein molecular weight marker (Bio-Rad). The Rf values of protein MW marker are shown in Table 8. The calibration curve of Log protein size (y-axis) versus relative mobility (Rf) (x-axis) is shown in Fig 42. The linearity of log MW of the marker was in the range of 25 kDa-100 kDa. The equation was

$$\text{Log molecular weight} = -0.9773 \times Rf + 2.15$$

The distance of PI was 2.05 cm, of PII was 3.50 cm, and the migration front was 5.0 cm. Therefore the Rf of PI was 0.39 and the Rf of PII was 0.68. The molecular weight of PI and PII were then determined from the calibration equation and showed that, the molecular weight of PI from SDS-PAGE gel was 58.7 kDa, whereas those of PII was 30.6 kDa.

Table 8 Rf value of proteins from SDS-PAGE gel

MW of protein marker (kD)	Distance (cm)	Rf
225	0.35	0.07
150	0.55	0.10
100	0.95	0.18
75	1.30	0.25
50	2.10	0.40
35	2.90	0.55
25	3.85	0.73
PI	2.05	0.39
PII	3.50	0.68

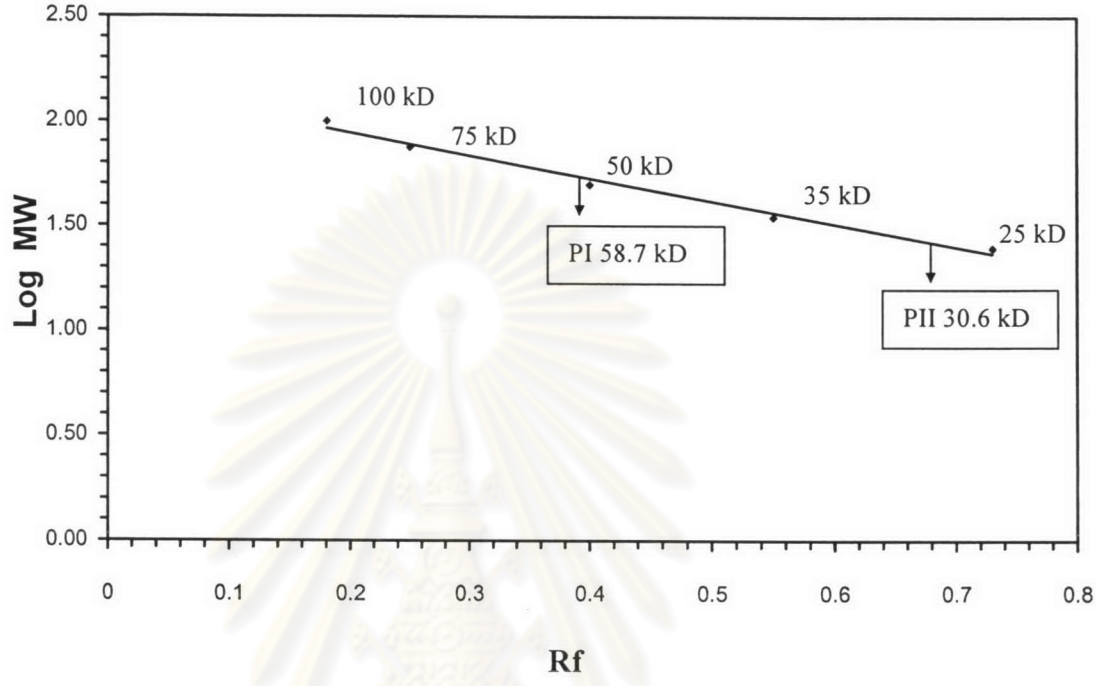

Figure 42 Standard calibration curve of Log molecular weight plotted against Rf values of standard proteins from 12% SDS-PAGE

3.2 Determination by Superose 6 gel filtration

The native form of enzyme was determined by Superose 6 column compared with the standard protein for gel filtration (Bio-Rad). The elution profile of standard proteins is shown in Fig. 43. The calibration curve of log molecular weight (x-axis) versus Vo/Ve (y-axis) was plotted (Fig. 44). The equation from the calibration curve was

$$\text{Log molecular weight} = 8.0564\ x - 2.2537$$

Vo of the column was 33.3 ml, PI was eluted out at 58.07 ml, while PII was eluted out at 70.5 ml.

The elution volume of the standard proteins is shown in Table 9.

Table 9 Vo/Ve value of proteins from Superose 6 gel filtration column

Peak	Protein	MW (kD)	Elution vol. (ml)	Vo/Ve
A	- (void peak)	-	33.3	1
B	thyroglobulin	670	53.4	0.62
C	gamma globulin	158	65.9	0.50
D	ovalbumin	44	69.5	0.47
E	myoglobulin	17	78.3	0.42
F	vitamin B12	1.35	93.4	0.36
	PI	232.4	58.07	0.57
	PII	34.1	70.5	0.47

As shown in Table 9, the molecular weights of PI and PII were calculated from the calibration curve. It was revealed that PI was 232.4 kD, whereas PII was 34.1 kD.

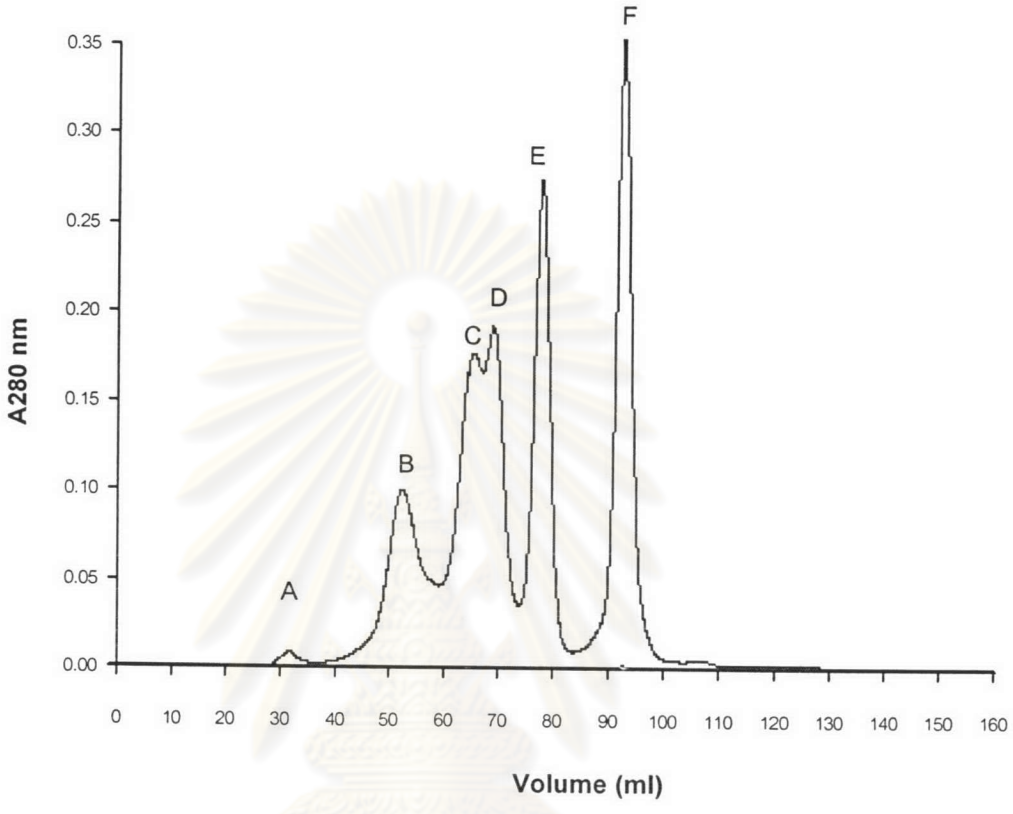

Figure 43 Elution profile of Bio-Rad molecular weight standard on superose 6 column. Peak A: void peak; B: thyroglobulin, 670 kD; C: gammaglobulin, 158 kD; D: ovalbumin, 44 kD; E: myoglobin, 17 kD; F: vitamin B_{12}, 1.35 kD.

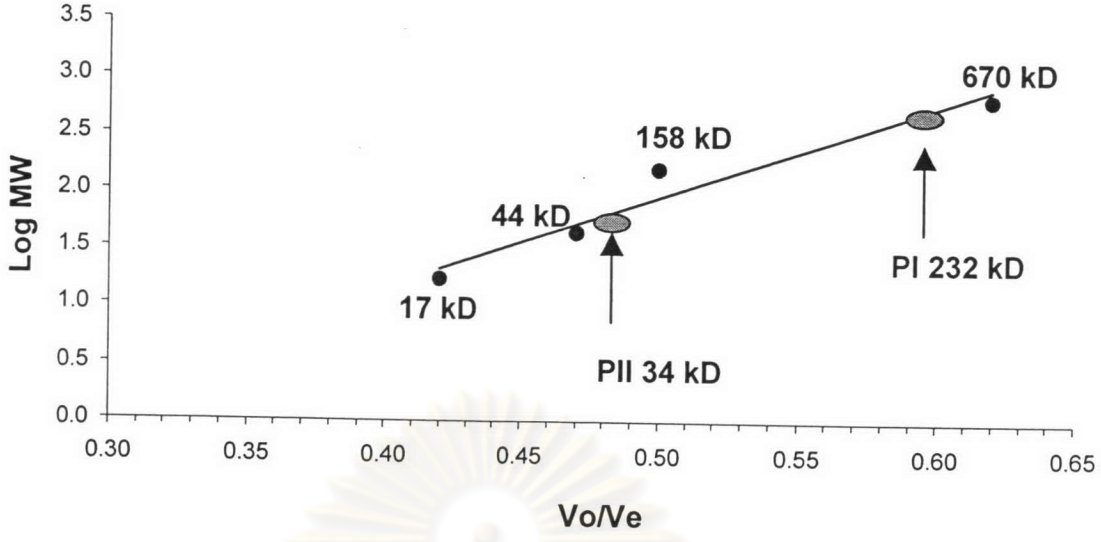

Figure 44 Standard calibration curve of Log molecular weight plotted against Vo/Ve of Superose 6 column.

4. Characterization of GGDP phosphatase

4.1 Kinetic studies of GGDP phosphatase of PI and PII

The primary plot according to the method of Michaelis-Menten was plotted between GGDP concentration (mM) and velocity of activity of PI and PII (pkat/mg) to obtain the rectangular hyperbolar graph as shown in Fig. 45 A. It was converted to Lineweaver-Burk which was the plot between 1/GGDP and 1/velocity to obtain *K*m and *V*max. The results showed that the *K*m value of PI was 0.2 mM, and the *V*max value of PI was 277.8 pkat/mg. No substrate inhibition was observed.

For PII the *K*m value was 0.1 mM, and the *V*max value was 7530 pkat/mg (Fig. 45 B). The velocity of PII showed 27-fold more than that of PI. The GGDP phosphatase activity of PII showed the substrate inhibition at concentration of GGDP more than 0.2 mM.

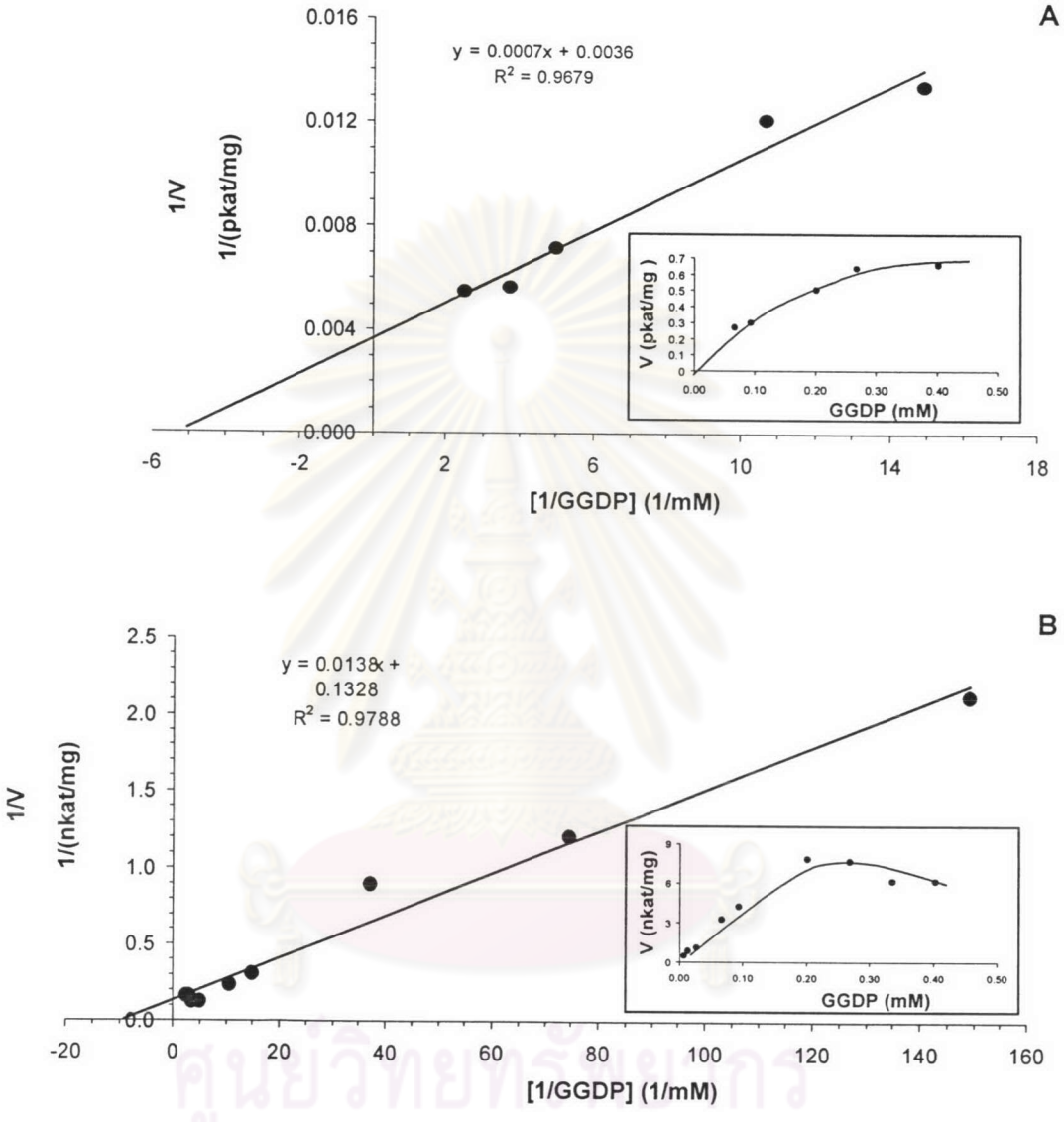

Figure 45 Lineweaver-Burk plot of GGDP phosphatase activity of PI (A) and PII (B) against GGDP concentration. Insert: Michaelis-Menten plot.

4.2 Influence of metal ions on the enzyme activity

The influence of metal ions on the enzyme activity of PI and PII was determined by performing the standard assay in the presence of 1 mM of $MnSO_4$, $CoCl_2$, Na_2MoO_4, $ZnSO_4$, $MgCl_2$ and $MnCl_2$ compared with standard assay without metal ion. The results are shown in Table 10, revealed that the activity of PI has less effect from the metal ion than that of PII. The activity of PI was decrease by Mn^{2+}, whereas the activity of PII was inhibited by Mn^{2+}, Zn^{2+}, and Co^{2+}. Both PI and PII activities were completely inhibited by 1 mM Na_2MoO4, which is a general phosphatase inhibitor.

Table 10 The influence of metal ions on the enzyme activity

Substances (1 mM)	% activity of PI	% activity of PII
Boiled control	0	0
No substance	100	100
$MgCl_2$	117	105
$ZnSO_4$	103	0
$MnSO_4$	96	0
$MnCl_4$	89	0
KCl	82	111
$CoCl_2$	79	0
NaCl	77	95
Na_2MoO_4	0	0

4.3 Substrate specificity

GGDP was the best substrate for PI and PII. PI was specific to GGDP for the incubation time of one hour. Increasing of the incubation time of PI also exhibited phosphatase activity over GDP and FDP. PII can use the substrates of GGDP:FDP:GDP in the ratio 100:23:10 for the incubation time of one hr (Table 11).

Table 11 Substrate specificity of PI and PII.

Substrate (0.2 mM)	% Relative activity	
	PI*	PII**
GDP	7	10
FDP	11	23
GGDP	100	100

PI*: incubation time 18 hr; PII**: incubation time 1 hr

4.4 Inhibition of enzyme activity by geraniol (GOH), farnesol (FOH), and geranylgeraniol (GGOH).

GOH (C_{10}), FOH (C_{15}), and GGOH (C_{20}) were prenol and the enzymatic product of phosphatase, and all of them have related structure. The possibility of enzyme inhibition by prenols were studies by incubating standard enzyme assay in the presence of 200,000 dpm [1-^{3}H]GGDP, and 0.1 mM of GOH, FOH, or GGOH. The peak of [1-^{3}H]GGOH was detected by TLC radioscanner. The control performed with boiled enzyme showed no peak of [1-^{3}H]GGDP, whereas the control with the absence of prenol showed no different amount of [1-^{3}H]GGDP. The results indicated that GOH, FOH, and GGOH had no effect to GGDP phosphatase activity of both PI and PII.

4.5 pH dependency of the enzyme activity

The relationship between pH and enzyme activity of PI and PII was determined within the pH capacity of various buffers as shown in Fig. 46. PI and PII exhibited enzyme activity in the pH range of 4.5-8.0.

PI activity was determined with 0.5 M Na_2HPO_4/citric acid buffer (pH 4.0, 5.0, 6.0), 0.5 M citric acid/sodium citrate buffer (pH 4.0, 4.5, 5.0), 0.5 M MOPS (pH 5.5, 6.0, 6.5, 7.0, 7.5, 8.0), and 0.5 M Tris/HCl (pH 7.0, 7.5, 8.0). The result shown in Fig. 46 A indicated that the optimum pH of PI was 6.0-6.5.

PII activity was determined with 0.5 M Na_2HPO_4/citric acid buffer (pH 4.0, 4.5, 5.0, 6.5), 0.5 M MOPS (pH 6.0, 6.5, 7.0, 7.5, 8.0), 0.5 M glycine (pH 7.5, 8.0, 8.5), and 0.5 M Tris/HCl (pH 7.0, 7.5, 8.0). The result shown in Fig. 46 B indicated that the optimum pH of PII was 6.5-7.0.

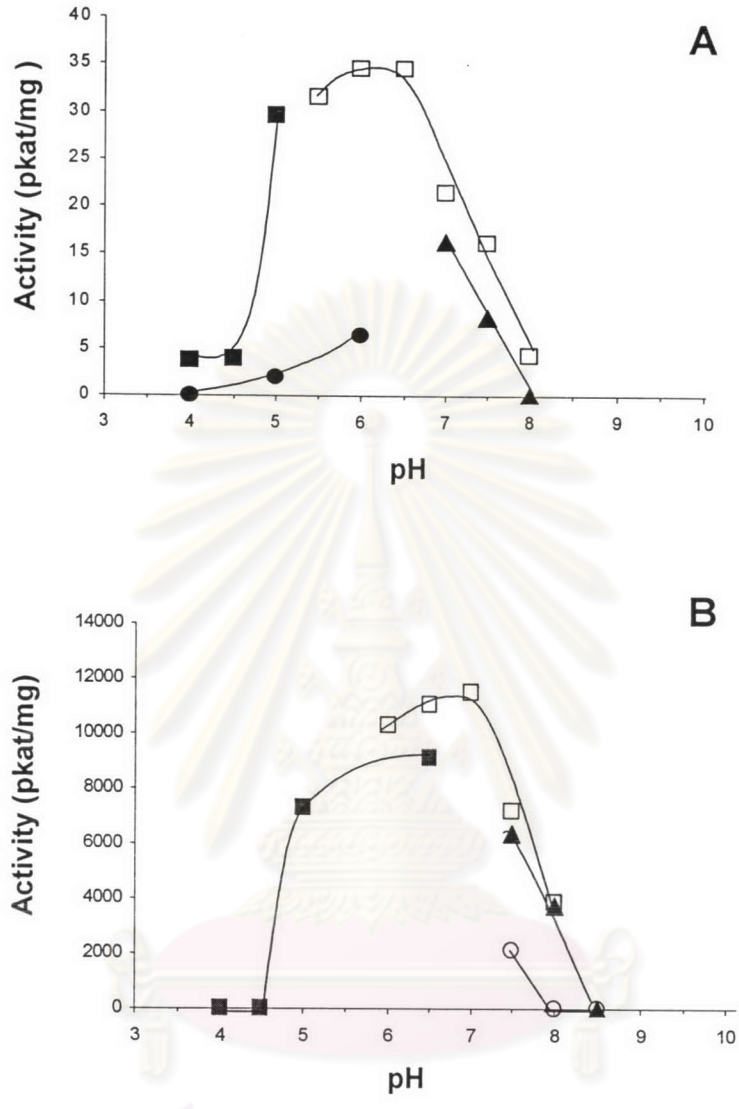

Figure 46 Effect of pH on GGDP phosphatase activity of PI (A) and PII (B) (•) Na_2HPO_4/citric acid, (□) MOPS buffer, (▲) Tris/HCl buffer, (O) glycine buffer.

5. Dephosphorylation step of GGDP by PI and PII

The consequence step of dephosphorylation reaction was determined. The GGMP was detected as an intermediate of reaction. Using solvent system of isopropanol-NH_4OH-H_2O (6:3:1) can separate GGDP, GGMP and GGOH with the Rf values 0.2, 0.6, and 0.9, respectively. PI from Superose 6 ,and PII from UNOQ were incubated with 0.1 μCi [1-^{3}H]GGDP, in 0.5 M Tris/HCl pH 7.0, overnight. The result was shown in Fig. 47 revealed the present of GGMP and GGOH as the enzymatic products. It could be suggested that dephosphorylation of GGDP by PI and PII consisting of two steps. First, GGDP was cleaved one phosphate out to obtain GGMP, then the second phosphate group was cleaved to yield GGOH. The result in Fig. 48 showed the dephosphorylation of GGMP to obtain GGOH by PII from BiogelA, confirmed that GGMP was an intermediate of the phosphatase activity of PII.

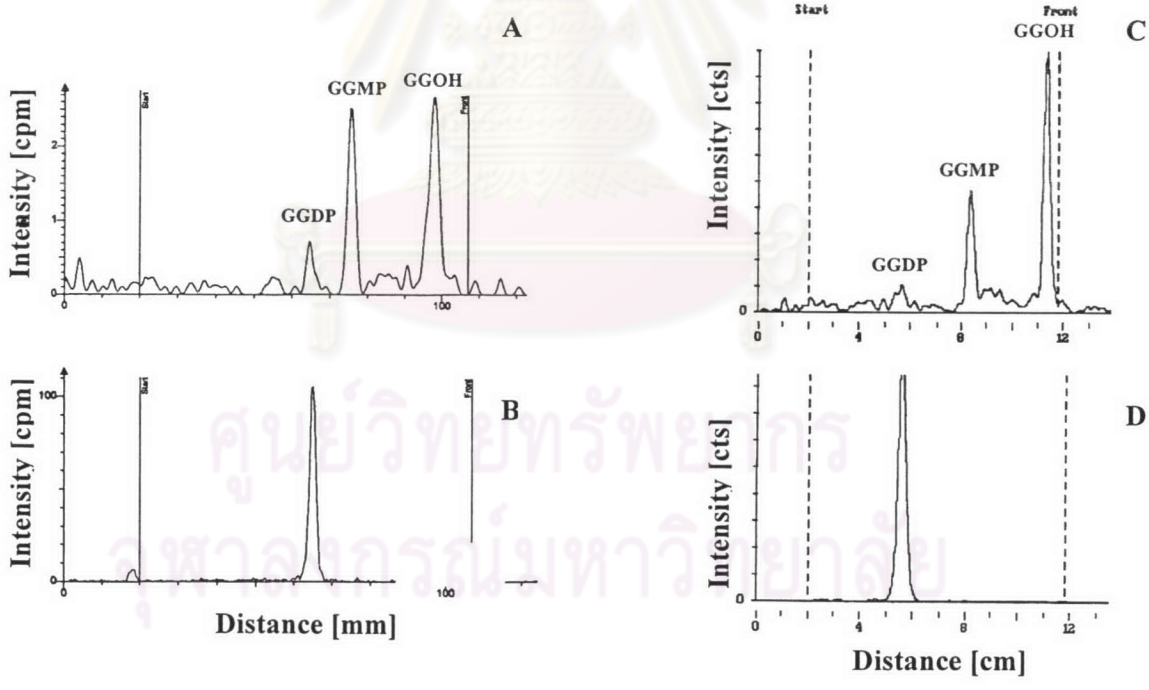

Figure 47 TLC radiochromatogram of dephosphorylation using [1-3H]GGDP as substrate. (A) dephosphorylation of PI from Superose 6 column; (B) boiled control of PI; (C) dephosphorylation of PII from UNO Q column; (D) boiled control of PII.

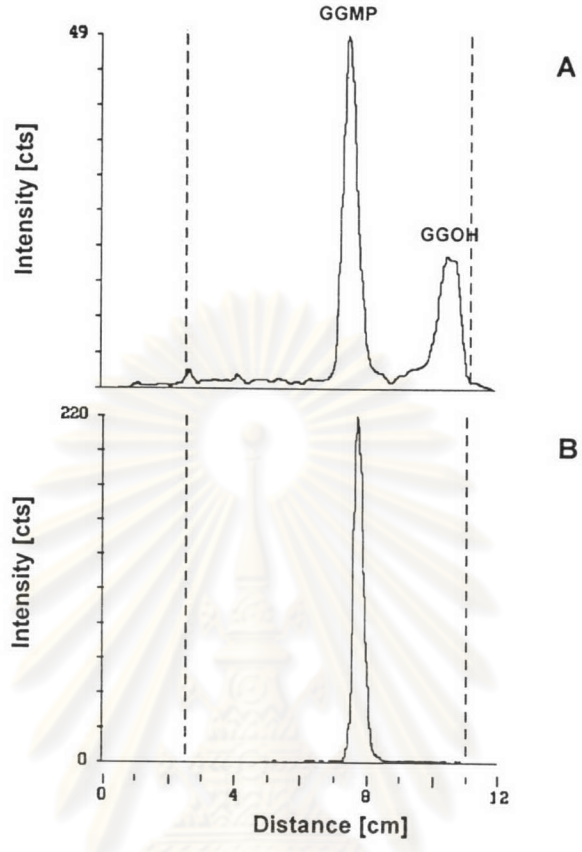

Figure 48 TLC radiochromatograms of dephosphorylation using [1-^{3}H]GGMP as substrate. (A) dephosphorylation of PII from BioGel A column; (B) reaction without enzyme.

4. Gene cloning of prenyl diphosphate phosphatase from *C. stellatopilosus*

1. Designed of degenerate primers

The amino acid sequences for prenyl diphosphate phosphatase were searched from database. The degenerated primers were designed from the consensus among prenyldiphosphate phosphatase (Lipid phosphate phosphatase, phosphatidic acid phosphatase) from *Arabidopsis thaliana* AtPAP1 (Q9ZU49), AtPAP2 (Q9X160), AtPAP3 (Q8LFD1), phosphatidic acid from *Oryza sativa* (Q8RZ97), phosphatidic acid of *Vigna unguiculata* (Q9FVL1), and diacylglycerol pyrophosphate phosphatase from *A. thaliana* (Q8LAS9).

Six degenerated primers were designed as shown in Table 12.

Table 12 Degenerated primers designed from prenyldiphosphate phosphatase

Sequences	Degenerated primers
1. HMHDWLI	5' CA(CT) ATG CA(CT) GA(CT) TGG (CT)T(AGCT) AT(ACT) 3'
2. DMMTDL	5' GA(CT) ATG ATG AC(AGCT) GA(CT) (CT)T(ACGT) 3'
3. DVYDLHH	5' GA(CT) GT(ACGT) TA(CT) GA(CT) (CT)T(AGCT) CA(CT) CA(CT) 3'
4. HTSWSF	5' (AG)AA (AGCT)(GC)(AT) CCA (AGCT)(GC)(AT) (AGCT)GT (AG)TG (AGCT)CC 3'
5. DDYWHHW	5' CCA (AG)TG (AG)TG CCA (AG)TA (AG)TC (AG)TC 3'
6. GWGPHAY	5' (AG)TA (AGCT)GC (AG)TG (AGCT)GG (AGCT)CC CCA(AGCT)CC 3'

Primer 4-6 were reverse complement nucleotide sequences (antisense direction).

Due to high homology among prenyl diphosphate phosphatase, lipid phosphate phosphatase and phosphatidic acid phosphatase, the amino acid sequences from those proteins were used to determine for the consensus regions. Moreover, all of them contained phosphatase motif.

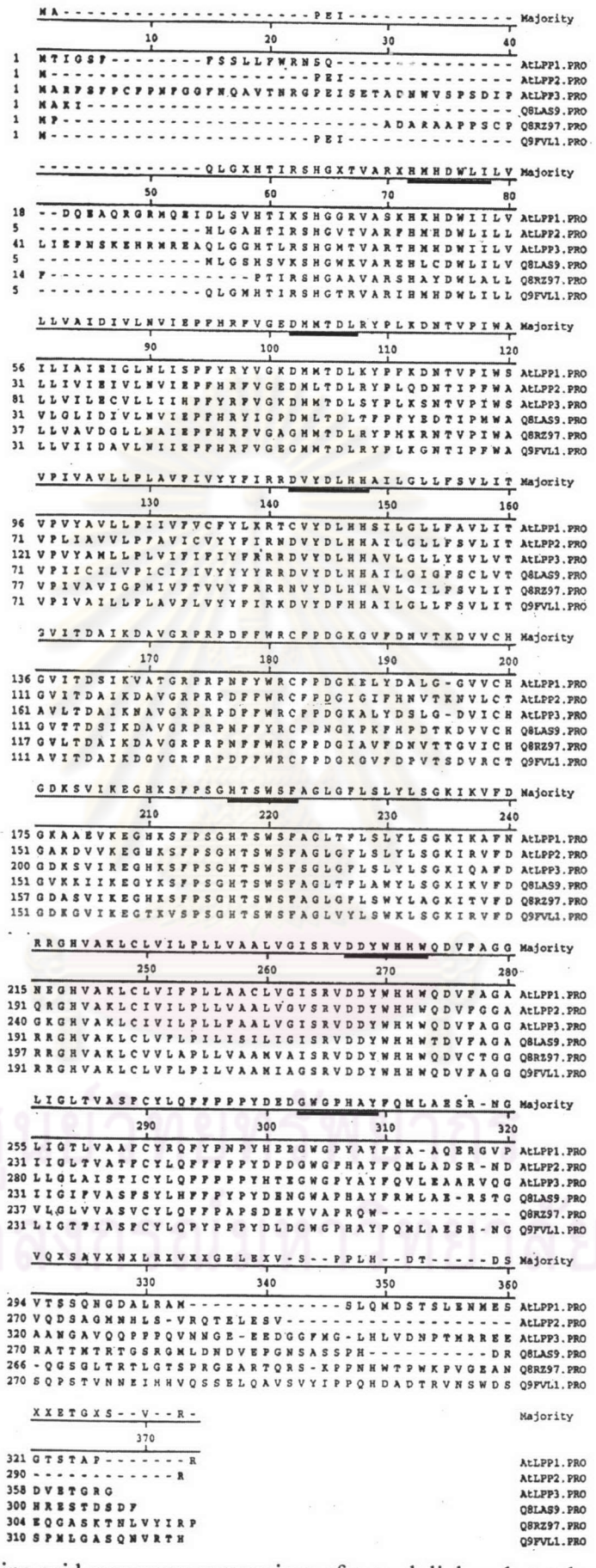

Figure 49 Amino acid sequences comparison of prenyl diphosphate phosphatases. The regions used for primer design were underlined.

2. Total RNA extraction

Young leaves of *C. stellatopilosus* (1 g) was used and total RNA was extracted by using phenol-chloroform method. The quality of total RNA was determined by agarose electrophoresis (Fig. 50) and its concentration was determined by UV spectrophotometry at wavelength of 260 nm. The yield of total RNA was 84.12 μg/g fresh leaves.

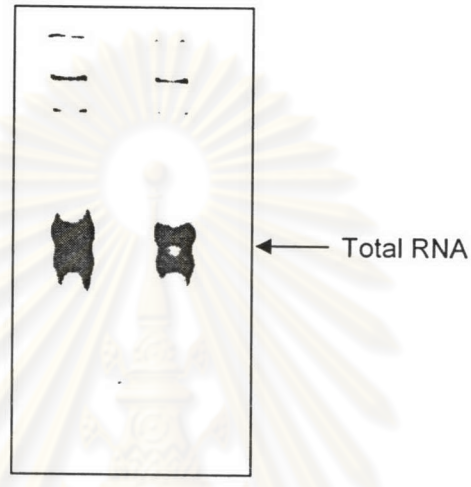

Figure 50 Agarose gel of total RNA from fresh leaves of *C. stellatopilosus*.

3. cDNA synthesis and PCR from degenerated primer

The first strand cDNA were synthesized from 5 μg total RNA by RT-PCR as described in part **3** of Materials and Methods. The PCR reaction mixture was performed with the template of total RNA and the primer of antisense direction (primer 4, 5, 6). The separated cDNA single strands of primer 4, 5, and 6 were obtained from the separated PCR .

Touchdown PCR was performed by using the first strand cDNA as template with the degenerated primer of sense and antisense direction. The combination of sense and antisense primers were varied. The amplicons showed multiple bands. The specific band was verified by Nested PCR using gradient temperature. The result in Fig.51 was obtained from touchdown PCR with degenerated primers 1 and 6, and template of single strand cDNA of primer 6, then the PCR product with multiple bands was used as template for Nested PCR with the second couple of primers 2 and 5. The single band of 512 bp nucleotides was obtained at the annealing temperature of 54.3 ^{O}C from gradient temperature.

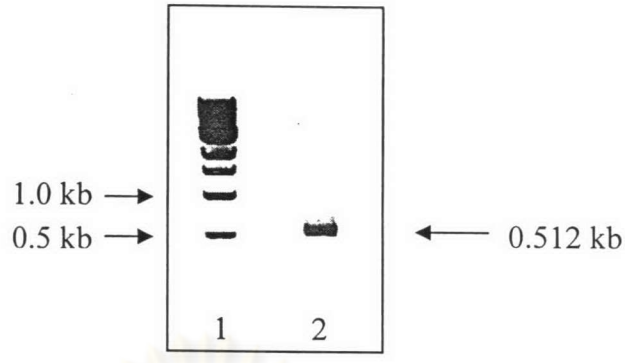

Figure 51 Agarose gel electrophoresis of Nested PCR product (lane 2) compared with 1 kb DNA ladder (lane 1).

4. Subcloning and sequence analysis of amplified PCR fragment

The PCR products were extracted from agarose gel, ligated into pGEM-T Easy vector, and transformed into competent *E.coli* DH5α. The single white colonies which contained gene insertion were picked up and grown in LB medium containing 1 μg/ml ampicilin to obtained more cells. The plasmid were isolated and analyzed for nucleotide sequences. The nucleotide sequences were identified by using TBLASTX program of the NCBI (http://www.ncbi.nlm.nih.gov). The results showed homology to phosphatidic acid phosphatases and prenyl diphosphate phosphatases.

5. Full-length gene

Based on the obtained sequence information of the putative 512 bp cDNA, new primers were designed overlapping between directed upstream of the 5′-end (primer 5′-RACE) and downstream of the 3′-end (primer 3′-RACE1, and 3′-RACE2).

The 5′-RACE and 3′-RACE PCR were performed as described in the method using the first strand cDNA which was synthesized according to the protocol. Three amplicons from 3 primers were obtained from touchdown PCR as shown in Fig. 52. Then they were analyzed for nucleotide sequences. The fragments were connected together by overlapping area of nucleotide. Full-length gene was obtained (Fig. 54). The open reading frame was determined from the starting codon of ATG to the stop codon of TAA.

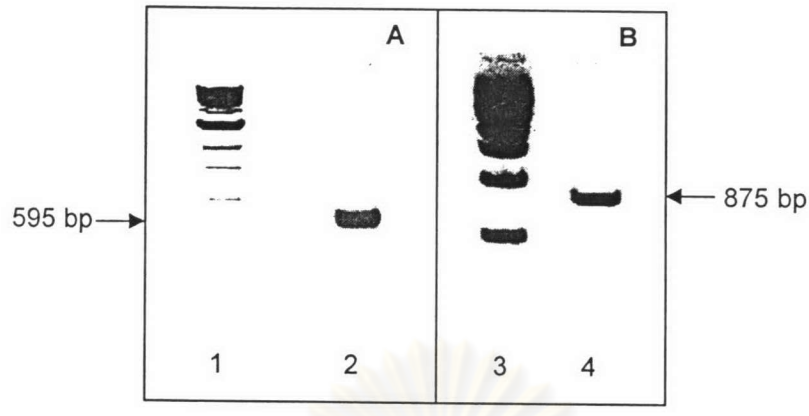

Figure 52 Agarose gel of touchdown PCR product of 3′-RACE and 5′-RACE. A) 5′-RACE PCR (595 bp); B) 3′-RACE1 (875 bp)

There are 2 possible positions of the open reading frame (ORF) with the same position of stop codon TAA. The first ORF (ORF1) of 888 bp started from nucleotide 85 to nucleotide 972, encodes a protein of 296 amino acids with a calculated molecular mass of 33.6 kD. The second ORF (ORF2) of 798 bp started from nucleotide 175 to nucleotide 972, encoded a protein of 266 amino acid with a calculated molecular mass of 29.9 kD. The nucleotide sequence and its deduced amino acid sequence were shown in Fig. 53. The full-length gene of ORF (ORF1, and ORF2) were further studies. The chloroplast transit peptide area of the deduced amino acid sequence of ORF1 and ORF2 were predicted by program ChloroP. The prediction revealed no chloroplast transit peptide available in both sequences of ORF1 and ORF2

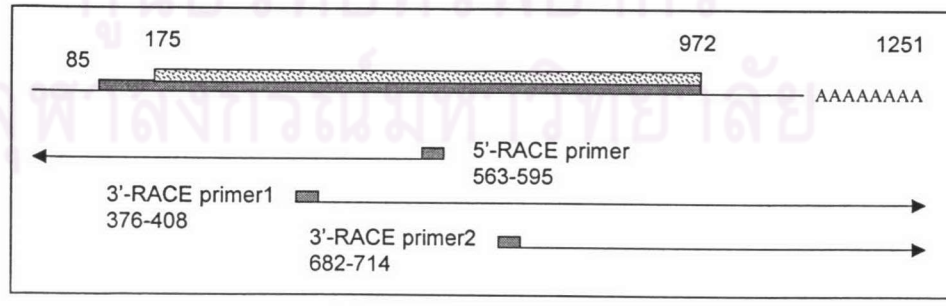

Figure 53 Diagram of RACE PCR fragment and the connection into full-length gene

```
1      atacaatgagtacaaagaggagggaggtccagcattggctcacatactgtgacgtcccat      60
61     ggagttgcagctgctaggacgcacATGCATGATTGGCTTATCTTTCTGCTTCTTGTGGTG      120
                                M  H  D  W  L  I  F  L  L  L  V  V -12
121    ATAGAGGTGATTTTATATGTTATTCATCCTTTTAAACGATATGCTGGGAAGGACATGATG      180
    13- I  E  V  I  L  Y  V  I  H  P  F  K  R  Y  A  G  K  D  M  M -32
181    ACAGATCTCAGATACCCTTTACAAAGTAATACGGTACCCGTTTGGGCAGTTCCAATGTAT      240
    33- T  D  L  R  Y  P  L  Q  S  N  T  V  P  V  W  A  V  P  M  Y -52
241    GCCATTCTTTTGCCAATGCTGGTTTTCCTAGTTGTCTATTTTCGTAGGAGAGACATCTAT      300
    53- A  I  L  L  P  M  L  V  F  L  V  V  Y  F  R  R  R  D  I  Y -72
301    GACCTCCATCATGCCATACTAGGTCTCTTTTATTCTGTTCTAGTCACAGCTGTAATTACT      360
    73- D  L  H  H  A  I  L  G  L  F  Y  S  V  L  V  T  A  V  I  T -92
361    GATTCGATAAAAAATGCAGTTGGCCGGCCTAGGCCTGATTTCTTTTGGCGCTGTTTTCCT      420
    93- D  S  I  K  N  A  V  G  R  P  R  P  D  F  F  W  R  C  F  P -112
421    GATGGAAAGGATGTTTATGATCAGCTGGGAAATGTTATATGCCATGGTGATAAAAATGTT      480
   113- D  G  K  D  V  Y  D  Q  L  G  N  V  I  C  H  G  D  K  N  V -132
481    ATAAAGGAAGGACACAAAAGTTTTCCAAGTGGGCATACTTCATGGTCCTTTGCTGGACTG      540
   133- I  K  E  G  H  K  S  F  P  S  G  H  T  S  W  S  F  A  G  L -152
541    GGGTTTTTGTCGCTTTACTTATCTGGGAAGTTGAAAGCATTTGACCGCAGAGGCCATGTT      600
   153- G  F  L  S  L  Y  L  S  G  K  L  K  A  F  D  R  R  G  H  V -172
601    GCAAAGCTATGTATCATCTTTCTTCCATTGCTAGTTGCTTGTCTTGTTGGCATTTCTCGA      660
   173- A  K  L  C  I  I  F  L  P  L  L  V  A  C  L  V  G  I  S  R -192
661    GTGGACGACTATTGGCATCATTGGCAGGATGTATTTGCTGGAGGTCTCTTAGGGCTCACG      720
   193- V  D  D  Y  W  H  H  W  Q  D  V  F  A  G  G  L  L  G  L  T -212
721    GTATCAACATTTTGTTATTTGCAGTTCTTCCCTCCACCATATCATCCTCAGGGTTGGGGG      780
   213- V  S  T  F  C  Y  L  Q  F  F  P  P  P  Y  H  P  Q  G  W  G -232
781    CCTTATGCTTACTTTCGGGTACTGGAGGAGTCCCATGGAAATACACAAGCATCTAGTGCT      840
   233- P  Y  A  Y  F  R  V  L  E  E  S  H  G  N  T  Q  A  S  S  A -252
841    ACAAATTTGCTAAATTCAGAGTCAAGAGTGGGTGAAGAAGAAGAAAGTAATGTATTTATG      900
   253- T  N  L  L  N  S  E  S  R  V  G  E  E  E  E  S  N  V  F  M -272
901    GGGCTACATTTAGCTCGCAACTCTAGTTTGCCAATGGAAAGCCACCAGGACGTTGAAAGG      960
   273- G  L  H  L  A  R  N  S  S  L  P  M  E  S  H  Q  D  V  E  R -292
961    GGACCAAAATAAtgtctagtaaaatcatagaaaggctcaggttgacaagaaggaaaatat     1020
   293- G  P  K  .
1021   tgcatcttattgcttattattactgtccaagttacaatcactcggatgcaggaagtttta     1080
1081   atgtagcatttttgtaaatgatggggtgcactgtggtgaaattaatggtatattccaat     1140
1141   tttaatctgcaggaaagtttttcccttaataatgtcggaattctgattctgctgtttgat     1200
1201   taacttattatattattcttgccttttcgaaaaaaaaaaaaaaaaaaaa  1251
```

Figure 54 Full-length gene of ORF1 and ORF2. The start codons were in bold letters.

5. Expression of *C. stellatopilosus* prenyl diphosphate phosphatase in *E. coli.*

In order to express *C. stellatopilosus* prenyl diphosphate phosphatase, the gene was constructed and cloned into the plasmid pET 101/D-TOPO vector. The primer was designed as shown in Material and Methods. The fusion protein with His-tag at C-terminal of ORF1, truncate of ORF1, ORF2, truncate of ORF2, and gene after RR motif had the calculated molecular weight of 37.1, 34.4, 33.4, 32.3, and 28.9 kD respectively. Fig. 55 showed the size of the fusion genes containing His-tag of such 5 clones with the sizes of 981, 915, 891, 864, and 777, respectively. The deduced amino acid and their truncate were shown in Fig. 56.

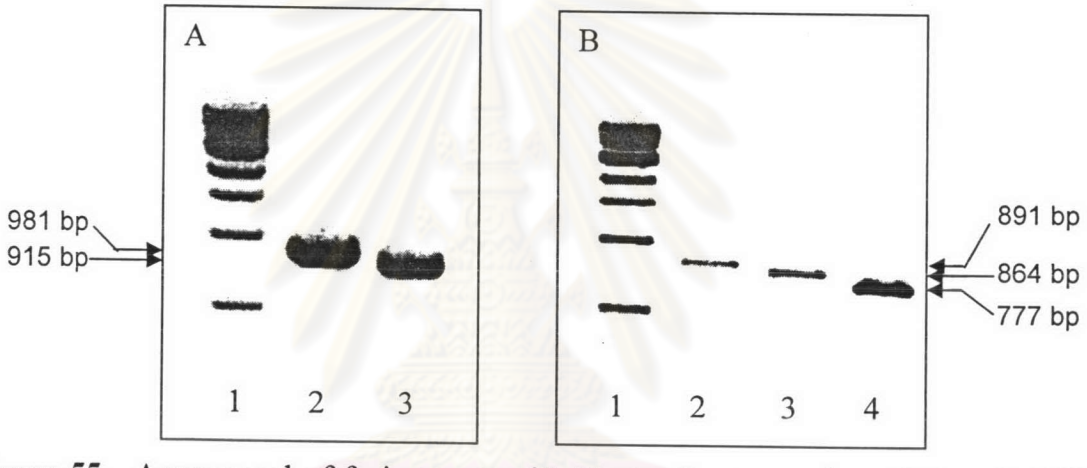

Figure 55 Agarose gel of fusion gene with his-tag for expression. A) lane 1: 1-kb DNA ladder; lane 2: ORF1; lane 3: ORF 2; B) lane 1: DNA ladder; lane 2: truncated ORF1; lane 3: truncated ORF2; lane 4: gene after RR motif .

1.	MHDWLIFLLLVVIEVILYVIHPFKRYVGKDMMTDLRYPLQSNTVPVWAVPMYAILLPMLVFLVVYFRRRDIYL
2.	MKRYVGKDMMTDLRYPLQSNTVPVWAVPMYAILLPMLVFLVVYFRRRDIYL
3.	MMTDLRYPLQSNTVPVWAVPMYAILLPMLVFLVVYFRRRDIYL
4.	MSNTVPVWAVPMYAILLPMLVFLVVYFRRRDIYL
5.	MDIYL
	HHAILGLFYSVLVTAVITDSIKNAVGRPRPDFFWRCFPDGKDVYDQLGNVICHGDKNVIKEGHKSFPSGHTSW SFAGLGFLSLYLSGKLKAFDRRGHVAKLCIIFLPLLVACLVGISRVDDYWHHWQDVFAGGLLGLTVSTFCYLQ FFPPPYHPQGWGPYAYFRVLEESHGNTQASSATNLLNSESRVGEEEESNVFMGLHLARNSSLPMESHQDVERG PKKGELNSKLEGKPIPNPLLGLDSTRTGHHHHHH.

Figure 56 Starting amino acid of 5 clones of *C. stellatopilosus* prenyl diphosphate phosphatase. 1 = ORF1, 2 = truncated ORF1, 3 = ORF2, 4 = truncated ORF2, 5 = sequence after RR motif. The following amino acid sequence was the same in all clones, with his-tag at C-terminal.

6. Purification of *C. stellatopilosus* prenyl diphosphate phosphatase by affinity column

The protein expression pattern from crude lysate cells showed two major bands. They seemed to be the recombinant proteins because of their appearances after induction by IPTG (Fig. 57,58). However, they were also contained in the flow through fraction from Talon resin column. So the recombinant proteins with his-tag were determined with His-tag monoclonal antibodies (His-tag Mab) as described in Materials and Methods. Proteins from SDS-PAGE gel were blotted into nitrocellulose membrane by electricity (Western Blot). The membrane was stained with Fast-green dye in order to locate the position of proteins before determination by using His-tag Mab. The positions of two major bands were marked. The results in Fig. 60 showed clearly that the major bands were not the His-tagged protein. The protein ORF1, truncated ORF1, ORF2, and truncated ORF2 showed obvious bands of interaction with His-tag Mab approximately 30 kDa positions. Protein after RR motif showed a different band as shown in Fig. 60. This might result from degradation of this protein. The ORF2 protein also showed a band approximately 66 kDa of MW, and it was appeared on SDS-PAGE gel. It might be a protein rich of histidine, so that it could bind to His-tag Mab.

It was difficult to identify the recombinant His-tagged protein bands by SDS-PAGE gel, eventhough the concentrated fraction from Talon resin column was loaded onto the gel and further stained with silver (Fig. 57,58). By comparison of MW position from nitrocellulose membrane in Fig. 59, the band of recombinant proteins in SDS-PAGE gel could be identified.

The purification of *E. coli* crude lysate from Co^{2+} binding affinity column (Talon resin column) showed several bands of proteins. So Ni^{2+} binding affinity Hi-trap^{R} column (Amersham) was tried. The proteins obtained from both column were not pure. The fractions from Hi-trap column was loaded into SDS-PAGE, staining with Coomasie blue. The band of the expression protein can be identified as shown in Fig. 59.

7. GGDP dephosphorylation of recombinant *C. stellatopilosus* prenyl diphosphate phosphatase

The fraction from Talon resin column was desalted by PD-10 column and concentrated by using Centricon-10. Then it was investigaed for GGDP phosphatase activity. The activity assay was performed with the control of the empty vector. The result in Fig 61 showed the GGDP phosphatase activity of all 5 proteins (ORF1, truncated ORF1, ORF2, truncated ORF2, and protein after RR motif). The main enzymatic product of ORF1 was of GGOH, whereas GGMP was the main product of other enzymes. However GGOH was also formed from ORF1 without cTP, protein ORF2, and protein ORF2 without cTP but in a small amount. (Fig. 61 and 62).

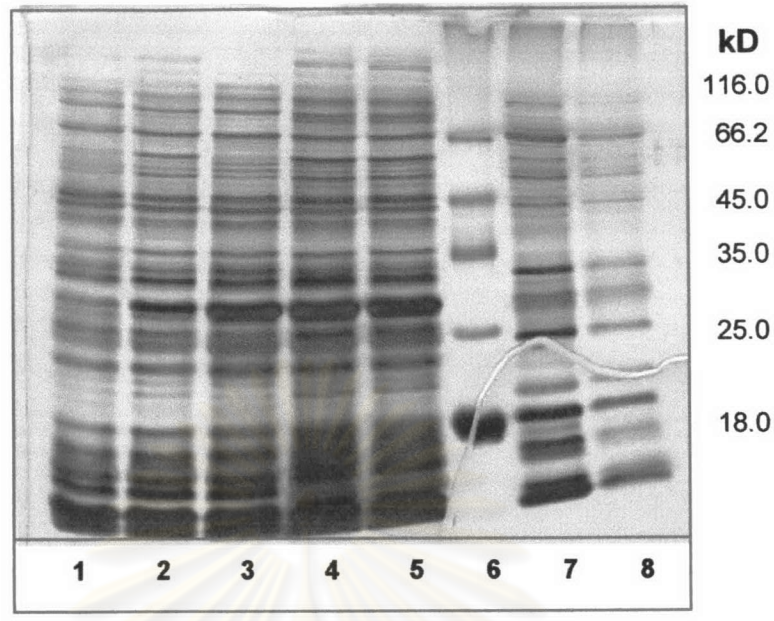

Figure 57 SDS-PAGE of truncated protein ORF2.

Lane 1: 0-hr induction; lane 2: 4-hr induction; lane 3: overnight induction; lane 4: crude lysate; lane 5: flow through fraction from Talon column; lane 6: MW marker; lane 7-8: Talon fraction concentrated with trichloroacetic acid. (silver stained)

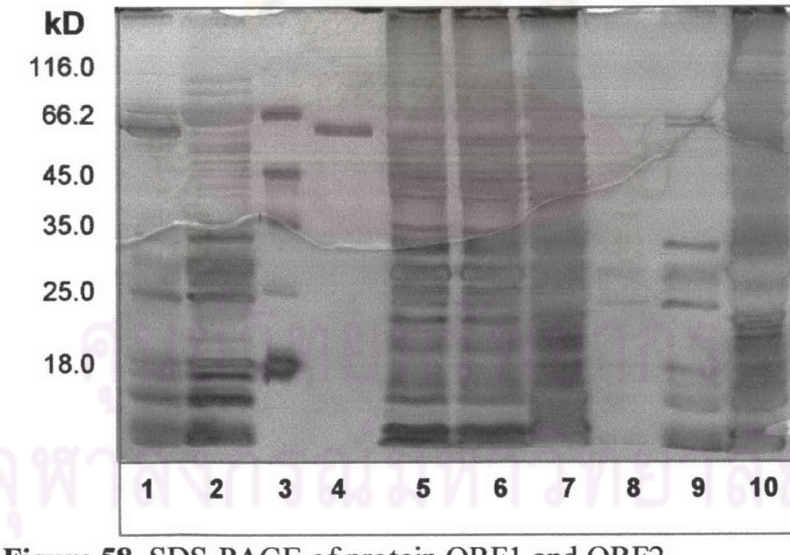

Figure 58 SDS-PAGE of protein ORF1 and ORF2.

Lane 1: Talon fraction of protein ORF2; lane 2,8,9: Talon fraction of protein ORF1; lane 3: MW marker; lane 4: Talon fraction of protein ORF2; lane 5: flow through fraction of protein ORF2; lane 6:crude lysate of protein ORF 2; lane 7: ORF 2 overnight induction; lane 10: crude lysate of protein ORF 1. (silver stained)

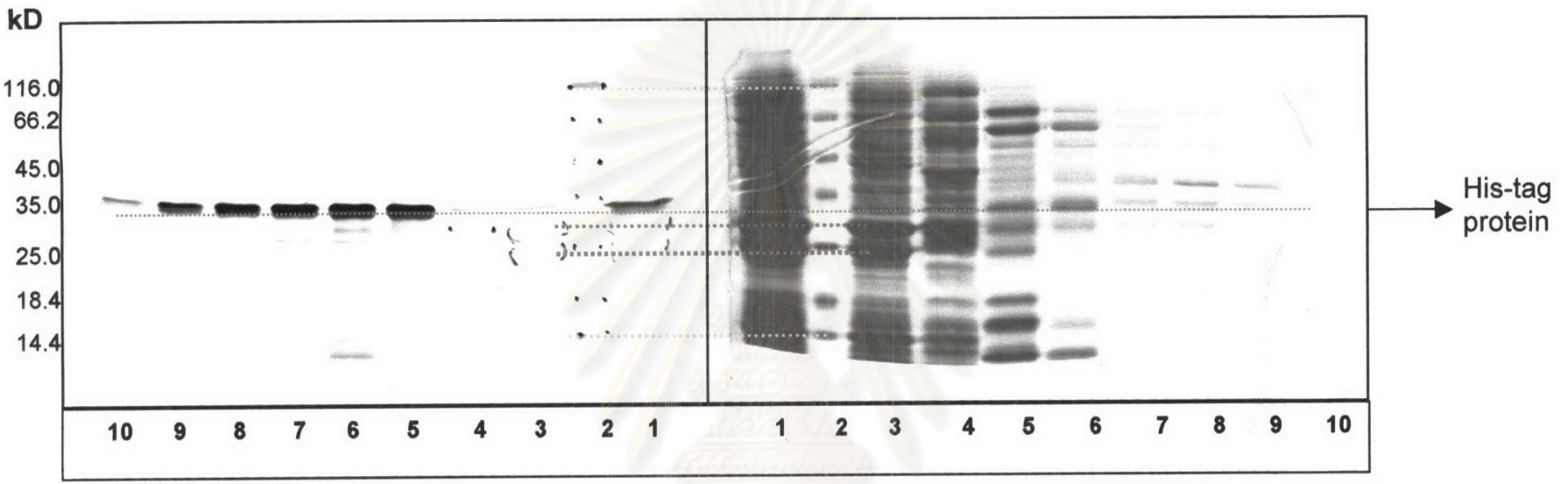

Figure 59 Western Blot of truncated ORF1 from HiTrap column (A) compared with SDS-PAGE (stained with coomasie blue) (B). Lane 1: crude lysate; lane 2: protein molecular weight marker; lane 3: flow through fraction; lane 4-10: fractions from Hi-Trap column.

(From A, lane 1, 5-9 showed band against His-tag monoclonal antibodies. The lines under his-tag protein in lane 1, and dots in lane 2-4 are pencil.

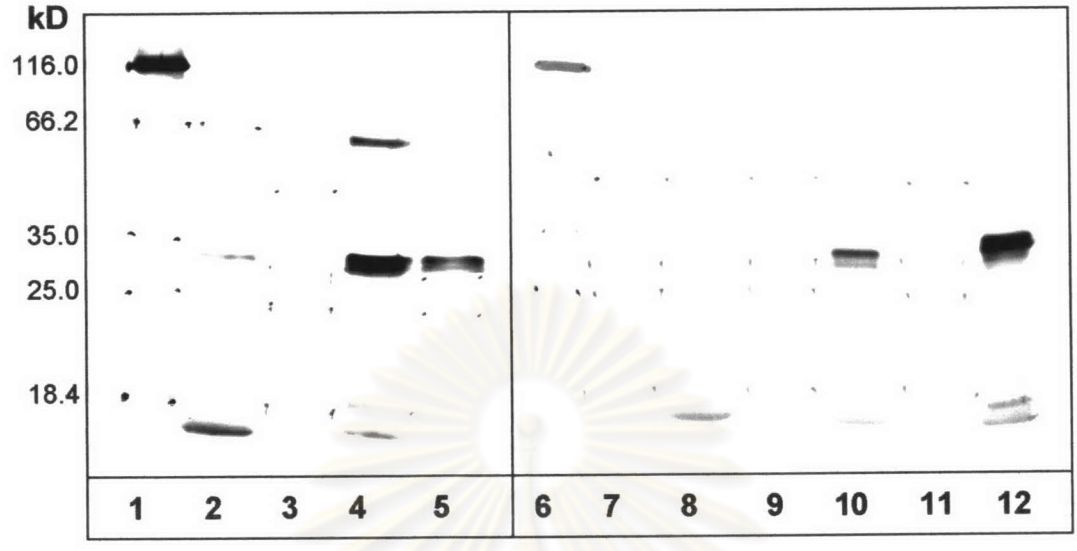

Figure 60 Western Blot of recombinant His-tagged proteins from TALON resin column. The protein was concentrated with Centricon-10 before loading onto the gel. Lane 1 and 6: protein molecular weight marker; lane 2: protein ORF1; lane 3: flow through fraction of ORF1; lane 4: protein ORF2; lane 5: flow through fraction of ORF2; lane 7: flow through fraction of protein after RR motif; lane 8: protein after RR motif; lane 9: : flow through fraction of truncated protein of ORF2; lane 10: truncated protein of ORF2; lane 11: flow through fraction of truncated protein of ORF1; lane 12: truncated protein of ORF1.

The dots in the position below the bands in lane 3, 5, 7, 9, and 11 were the major bands in the flow through fraction from Talon resin column.

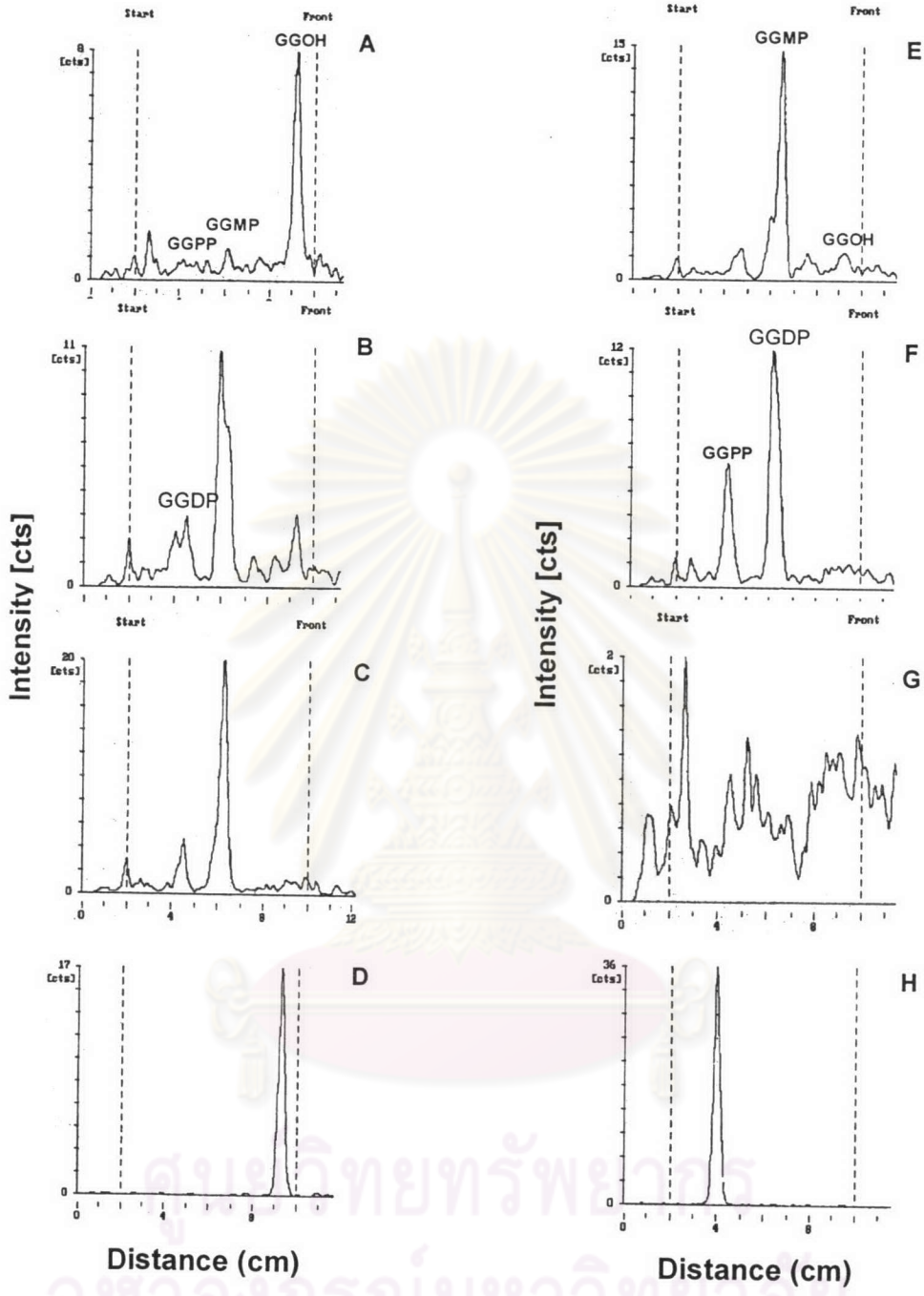

FIGURE 61 TLC radiochromatograms of the dephosphorylation of recombinant prenyl diphosphate phosphatase. The enzymatic product was applied on TLC silica gel plate with the solvent system of isopropanol-NH_4OH-H_2O (6:3:1). A) protein ORF1; B) protein of truncated ORF1; C) protein ORF2; D) standard [1-^{3}H]GGOH; E): protein of truncated ORF2; F) : protein after RR motif; G) empty vector control; H) standard [1-^{3}H]GGDP.

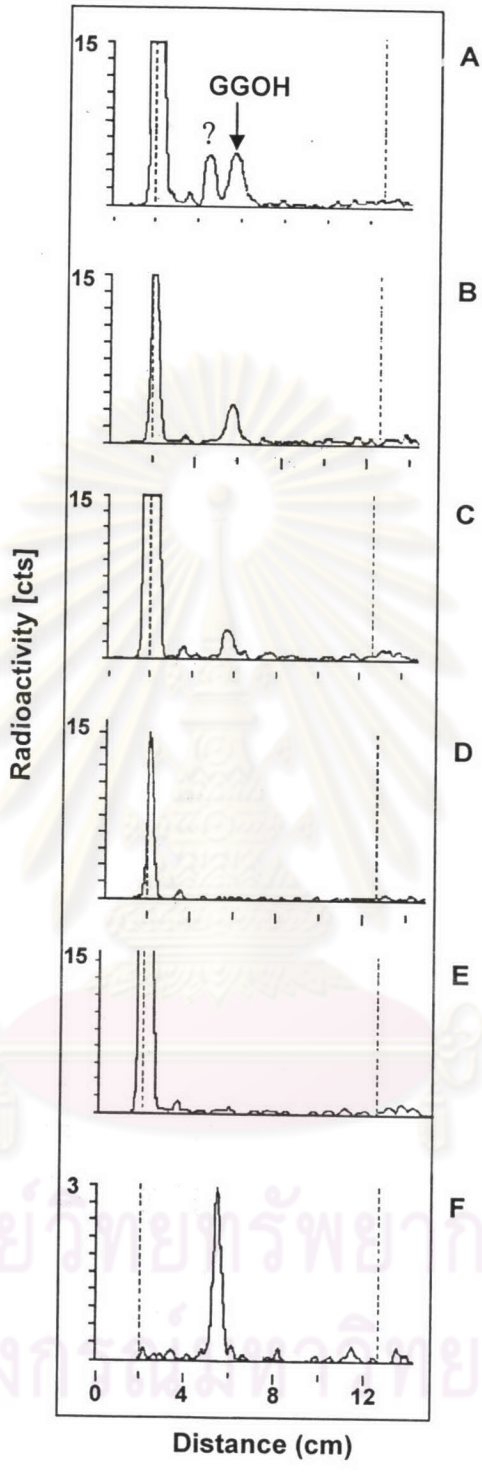

Figure 62 TLC radiochromatograms of the dephosphorylation activity of recombinant prenyl diphosphate phosphatase. A) protein ORF1; B) protein of truncated ORF1; C) protein ORF2; D) protein after RR motif; E) control *E.coli* with empty vector; F) standard [1-^{3}H]GGOH.